TABLE OF CONTENTS (TOC)

Modulation of Growth of Cysteine-capped Cadmium Sulphide Quantum Dots with Enzymatically produced Hydrogen Peroxide

Ruta Grinyte, Javier Barroso, Laura Saa, Valeri Pavlov*

Biofunctional Nanomaterials Unit, CIC BiomaGUNE, Parque Tecnológico de San Sebastian, Paseo Miramón 182, Donostia-San Sebastián, 20009 Spain

Page Numbers. The font is ArialMT 16 (automatically inserted by the publisher)

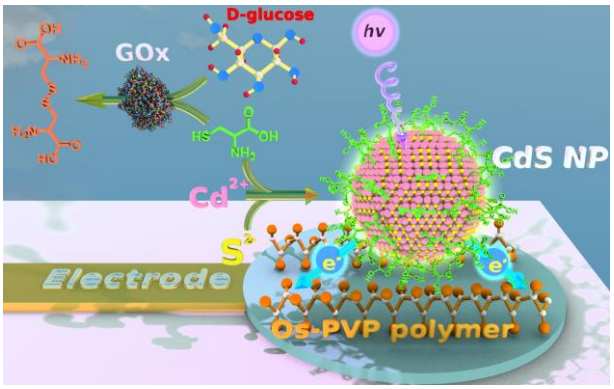

Enzymatically produced hydrogen peroxide oxidizes cysteine modulating the growth of quantum dots. This system allows quantification of glucose oxidase and glucose in human serum, using fluorescence spectroscopy and photoelectrochemical analysis.

Nano Res
DOI (automatically inserted by the publisher)
Review Article/Research Article **Please choose one**

Modulation of Growth of Cysteine-capped Cadmium Sulphide Quantum Dots with Enzymatically produced Hydrogen Peroxide

Ruta Grinyte[1], Javier Barroso[1], Laura Saa[1], Valeri Pavlov[1] ✉

[1] Biosensing Unit, CIC BiomaGUNE, Parque Tecnológico de San Sebastian, Paseo Miramón 182, Donostia-San Sebastián, 20009 Spain

Received: day month year / Revised: day month year / Accepted: day month year (automatically inserted by the publisher)

ABSTRACT

Cysteine (CSH) readily stabilizes CdS quantum dots (QDs) growing in aqueous buffered solutions. Oxidation of CSH by hydrogen peroxide (H_2O_2) at room temperature yields cystine (CSSC) which does not stabilize CdS QDs so efficiently as CSH does. Here we demonstrate that such oxidation causes the decrease in the rate of the formation of CSH - capped CdS QDs from Cd^{2+} and S^{2-} ions. For the first time, we combined the oxidation of CSH with biocatalytic oxidation of D-glucose catalyzed by glucose oxidase (GOx) leading to the buildup of hydrogen peroxide in the reaction mixture. Enzymatically modulated growth of CdS QDs in situ was monitored by two techniques: fluorescence spectroscopy and photoelectrochemical (PEC) analysis. This system allowed quantification of GOx and glucose in human serum.

KEYWORDS

quantum dots, photoelectrochemistry, enzyme, fluorescence, hydrogen peroxide

1. Instruction

The unstoppable development of nanotechnology during the last decades has allowed for the fabrication of new materials and design of novel biosensing methods. One of the valuable tools employed in biosensing are inorganic nanoparticles (NPs). NPs of noble metals like gold and silver exhibit high extinction coefficients due to surface plasma resonance [1]. The optical properties of metal NPs depend on their shape and size [2]. Traditionally metal NPs were used in bioanalysis as labels in affinity assays [3-5]; enhancers of raman scattering [6-9]; quenchers of fluorescence [10, 11] and scaffolds for assembling of biorecognition elements [12, 13]. Metal NPs can be produced in

Address correspondence to Valeri Pavlov, vpavlov@cicbiomagune.es

situ with biocatalytic processes catalyzed by different enzymes, for instance, glucose oxidase (GOx), alkaline phosphatase (ALP), and alcohol dehydrogenase (AlcDH) [14-16]. Metal NPs generated in situ by enzymes usually are not fluorescence and hardly demonstrate photocatalitic activities. This feature limits their employment in bioassays.

NPs composed of semiconductor materials demonstrate quantum effects and can be photoexcited emitting photons during the relaxation process. Therefore, those particles are referred to in the literature as quantum dots (QDs). They find broad application in nanotechnology, diagnostics and therapy [1, 17-20]. The energy of the emitted photons and consequently the intensity and the wavelength of the observed fluorescence depend on the nature and the shape of QDs, the environment and capping agents (stabilizers).

Cysteine (CSH), which carries thiol functional group for binding at CdS interface and hydrophilic amino and carboxylic groups, is an efficient stabilizer of CdS NPs [21, 22]. On the other hand, CSH can be easily oxidized to form a dimer containing disulfide bridge between two CSHs, known as cystine (CSSC). Oxidation of CSH with hydrogen peroxide (H_2O_2) in aqueous buffers can be described by the two-step nucleophilic reaction model [23-25]. This process is initiated by rate-determining nucleophilic attack of thiolate anion (CS^-) on unionized H_2O_2 to generate sulfenic acid (CSOH) as an intermediate product (Equation 1). The latter interacts with CS^- ions to yield CSSC as shown in equation 2.

$$CS^- + H_2O_2 \rightarrow CSOH + HO^- \quad (1)$$

$$CSOH + CS^- \rightarrow CSSC + HO^- \quad (2)$$

For the first time, we combined this reaction with biocatalytic oxidation of D-glucose (glucose) catalyzed by GOx leading to the buildup of H_2O_2 in the reaction mixture. GOx is the protein composed of two identical 80 kDa subunits containing two bound FAD coenzymes. Chemical, pharmaceutical, food, beverage, clinical chemistry, biotechnology and other industries broadly employ GOx [26]. The determination of GOx enzymatic activity is quite important in industry. The standard assay for GOx activity relies on the reaction mixture containing the additional enzyme horseradish peroxidase (HRP) that is used for detection of H_2O_2 produced by GOx (enzymatic assay of GOx from Sigma-Aldrich).

In the present work we demonstrate that the oxidation of the stabilizing agent CSH by H_2O_2 produced by GOx causes the decrease in the rate of the formation of CSH-capped CdS QDs from Cd^{2+} and S^{2-} ions. This process allows relating the enzymatic activity of GOx and glucose concentration with amount of CdS QDs produced in situ which defines the emission spectrum of the assay mixture followed by the fluorescence spectroscopy, the extremely sensitive laboratory technique for detection of the fluorescence readout signal.

We also used the powerful alternative to fluorometry, the photoelectrochemical (PEC) analysis [27, 28]. PEC sensors are becoming a promising low cost approach for the detection of light responsive chemical and biochemical molecules [29-31]. The process of PEC detection converts luminous energy into electrochemical energy at the surface of the electrode, generating electrical readout signal. The photocurrent intensity is defined by the characteristics of excitation light, applied potential and the rate of the electron transfer between the electron surface and QDs. A number of electrocatalysts have been applied to facilitate the electron transfer to the electrode surface in PEC analysis, such as microporous carbon including carbon nanotubes and grapheme [32], small organic molecules like methyl viologen immobilized on polymeric nafion matrix [33],

semiconductor metal oxides like TiO_2 [34]. Usually electrocatalysts were immobilized on expensive gold and indium tin oxide (ITO) electrodes using anchoring thiol and silane groups [35]. Screen-printed carbon electrodes (SPCE) are significantly cheaper but their modification with electrocatalysts is quite difficult due to the absence of anchoring functional groups on the surface of the carbon material of the working electrode. In the present work we employ the complex of poly(vinylpyridine) with $Os(bipyridine)_2Cl_2$ (Os-PVP complex) as the electrocatalyst to facilitate the electron exchange. Previously, the redox polymer of this structure was applied to wire redox enzymes, for instance, glucose-6-phosphate dehydrogenase [36] and HRP [37].

In this article we present a new strategy for detection of enzymatic activities using the fluorescent spectroscopy and PEC. We offer a quite universal bioanalytical platform relying on the enzymatically modulated growth of CdS QDs in situ followed by two techniques which finally will be applicable to the range of detection systems spanning from optical laboratory equipment to low power mobile fast point of care (POC) analytical systems.

2. Experimental

Materials. Sodium sulfide (Na_2S), cadmium nitrate $Cd(NO_3)_2$, glucose oxidase type VII from Aspergillus niger and other chemicals were purchased from Sigma Aldrich. Anhydrous ß-D-glucose and hydrogen peroxide (30% v/v) were purchased from Panreac.

Characterisation. *Spectroscopy.* Transmission electron miscroscopy (TEM) images were collected with a JEOL JEM 2100F operating at 120 kV.

Optical methods. Fluorescence measurements were performed on a Varioskan Flash microplate reader (Thermo Scientific) using black microwell plates at room temperature. The system was controlled by SkanIt Software 2.4.3. RE for Varioskan Flash.

Photoelectrochemistry. All electrochemical experiments were conducted in the Autolab Electrochemical Workstation (Model: PGSTAT302N, Metrohm Autolab, The Netherlands) equipped with NOVA 1.10 software. Disposable screen-printed carbon electrodes (SCPEs) were purchased from DropSens (model DRP-110, 4 mm diameter). Electrical contact to workstation was done with a special boxed connector supplied by DropSens. The illumination source was a compact UV illuminator (UVP, Analytik Jena AG). All PECs were performed at room temperature. All the potentials reported in our work were against Ag/AgCl. Unless mentioned otherwise, all experimental results presented here are averaged from three independent measurements (n = 3).

Methods CdS QD-mediated determination of H_2O_2. Different concentrations of H_2O_2 were incubated with 0.075 mM of CSH in citrate-phosphate buffer (pH 7.5) for 40 min at room temperature. After that, Na_2S (10 µL , 1 mM) and $Cd(NO_3)_2$ (2.5 µL , 50 mM) were added to the samples (87.5 µL). The emission spectra of the resulting suspensions were recorded after 5 min at λ_{exc} = 300 nm.

GOx assay. Varying amounts of glucose were incubated with different amounts of GOx in citrate-phosphate buffer (pH 7.5) for 40 min at room temperature, in the presence of CSH (0.075 mM). After that, Na_2S (10 µL, 1 mM) and $Cd(NO_3)_2$ (2.5 µL, 50 mM) were added to the samples (87.5 µL). The emission spectra of the resulting CdS QDs were recorded after 5 min at λ_{exc} = 300 nm.

Quantification of glucose in human serum. Quantification of glucose in human serum was performed by the standard edition method. Samples of pooled human serum (Sigma-Aldrich) were spiked with known different concentrations of glucose and the glucose concentration of the

mixtures was determined. The dilution factor of plasma in the assay was 1:100.

Photoelectrochemical detection. SPCEs were initially pretreated electrochemically by cyclic voltammetry (CV) at a potential range of 0 – 0.8 V in citrate-phosphate buffer (pH 7.5). Subsequently, a 40 μL drop of Os-PVP complex (1.375 mg mL^{-1}) was placed on the SPEs and deposited by CV scanning (2 cycles, 50 mV s^{-1}). Later, SPCEs were rinsed out with ultrapure water and dried under argon atmosphere. Finally, a 40 μL of samples were dropped on the SPCE and PEC measurements were carried out with UV illuminator at 365 nm and a controlled potential of 0.3 V. The dependence of photocurrent on time was measured at 5 minutes during 10 seconds. 1-thioglycerol (TG) was added to the samples to amplify the signal.

3. Results and discussion

3.1. CdS QD-mediated determination of H_2O_2 and optimization of the system

The ability of CSH to stabilize CdS QDs was studied. Cadmium nitrate ($Cd(NO_3)_2$) was interacted with sodium sulfide (Na_2S), in citrate phosphate buffer (pH 7.5) in the presence of CSH or CSSC, which is the oxidized form of CSH. The formation of fluorescent CdS QDs was followed by fluorescence spectroscopy. As one can see in Fig. 1 reaction mixture containing CSH, Cd^{2+} and S^{2-} ions demonstrated high emission peak (curve a). No significant fluorescence was observed in the presence of CSSC (curve b) or without any CSH and CSSC (curve c). This finding proves that CSSC does not stabilize fluorescent QDs so efficiently as CSH (Figure 1, curve b). In order to increase the yield of CSH-stabilized CdS NPs the effect of CSH concentration on fluorescence spectrum of the reaction mixtures containing Cd^{2+} and S^{2-} ions was investigated. According to Fig. S-1 Electronic Supplementary Material (ESM) optimum concentration of CSH was 0.075 mM, which was used in all subsequent experiments.

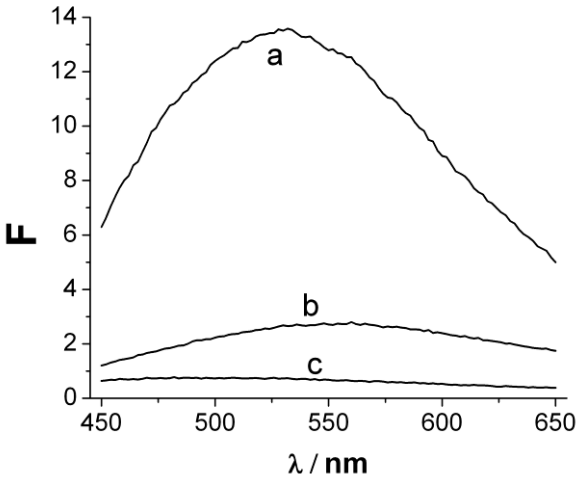

Figure 1. Fluorescence emission spectra of the system containing (a) CSH (0.5 mM), Na_2S (0.1 mM), $Cd(NO_3)_2$ (1.25 mM); (b) CSSC (0.5 mM), Na_2S (0.1 mM), $Cd(NO_3)_2$ (1.25 mM); (c) only Na_2S (0.1 mM) and $Cd(NO_3)_2$ (1.25 mM)

Thus, CSH is able to stabilize CdS NPs formed in situ from S^{2-} and Cd^{2+} ions in aqueous solutions within the incubation time of 5 min at room temperature (Scheme 1). The previously published procedures for the synthesis of CSH-stabilized CdS QDs required much longer incubation times (over 1 hour) and very harsh experimental conditions like high temperatures (over 80 °C) [22] or irradiation with γ-rays [21]. The process of CdS QDs formation under physiological conditions, optimized by us, was very rapid and compatible with natural biochemical pathways leading to oxidation of CSH for modulation of QDs' growth.

It was found out that the treatment of CSH with varying concentrations of H_2O_2 leads to the decrease in the rate of formation of CdS NPs due to

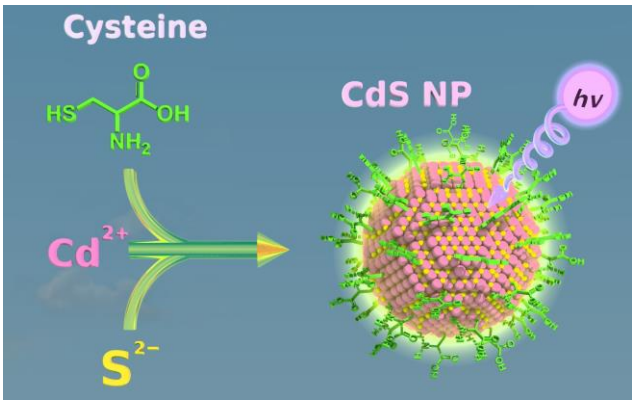

Scheme 1. Modulation of CdS QDs growth with cysteine.

oxidation of CSH into CSSC. As one can see in Fig. 2, the decrease in the fluorescence signal was directly related to the quantity of the H_2O_2 in the reaction mixture. Calibration curve shown in Figure 2 inset demonstrated linearity from 0.0 to 0.045 mM and saturation starting from 0.15 mM H_2O_2 concentration. In accordance with the calibration curve the limit of H_2O_2 detection (LOD) was calculated to be 12.6 μM by UPAC definition [38]. This LOD is 4 times lower than that of the reported most relevant fluorogenic assay for detection of H_2O_2 using the enzymatic growth of CdS NPs [39]. It is important to note that after addition of H_2O_2 (0.1 mM) to the pre-prepared CdS NPs stabilized with CSH no changes in the emission spectra of CdS NPs were noticed (Fig. S-2, curve b ESM). So, the decrease in the fluorescence was not caused by the possible quenching effect of H_2O_2. Transmission electron microscopy (TEM) was applied to confirm the existence of CSH stabilized CdS QDs in the reaction mixture at three different concentration of H_2O_2 (Fig. S-3 in the ESM). Analysis of the TEM images of CdS QDs revealed that the medium diameter of the produced NPs was 2.03 ± 0.32 nm in the absence of H_2O_2. When the concentration of H_2O_2 was 0.03 nm the observed CdS QDs exhibited the medium diameter of 1.29 ± 0.26 nm. In the presence of saturating concentration of H_2O_2 equal to 0.3 mM the absence of CdS QDs were confirmed by TEM.

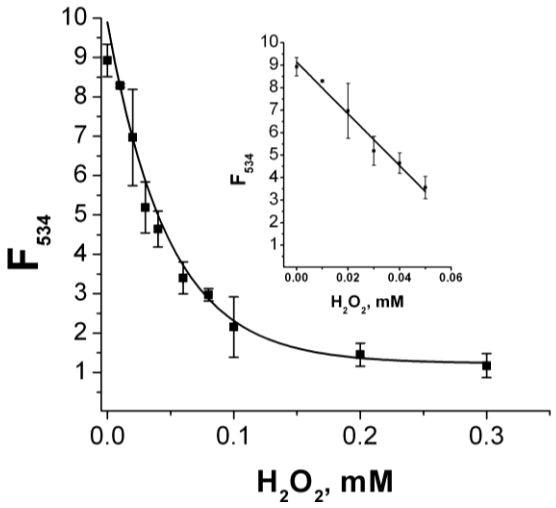

Figure 2. Calibration curve of H_2O_2 obtained using the intensity if the emission peak at 534 nm (F_{534}) The system containing of CSH (0.075 mM), Na_2S (0.1 mM) and $Cd(NO_3)_2$ (1.25 mM), and different concentrations of H_2O_2: a) 0 mM; b) 0.01 mM; c) 0.02 mM; d) 0.03 mM; e) 0.04 mM; f) 0.06 mM; g) 0.08 mM; h) 0.1 mM; i) 0.2 mM; j) 0.3 mM. Inset: linear part of the calibration plot.

3.2. Glucose oxidase assay

The above mentioned fluorogenic method for H_2O_2 detection can be readily combined with enzymatic reactions resulting in the formation of H_2O_2, for example oxidation of enzymatic substrates by oxidases. The operation principle of the fluorogenic assay for evaluation of enzymatic activity of GOx is represented in Scheme 2.

Oxidation of glucose with oxygen catalyzed by GOx ends up in the final products D-glucono 1,5-lactone and H_2O_2. Enzymatically produced H_2O_2 is able to oxidize CSH preventing stabilization and rapid formation of CdS QDs. Fig. 3 shows the emission spectra of CdS QDs formed in the presence of the fixed 1 mM glucose concentration and different concentrations of GOx. As one can see in Figure 3B, the increase in the amount of GOx leads to the decrease in the fluorescence signal as expected for this biocatalytic reaction. We calculated that the LOD of the system was 0.1 μg of GOx per mL. This assay showed 5 times better

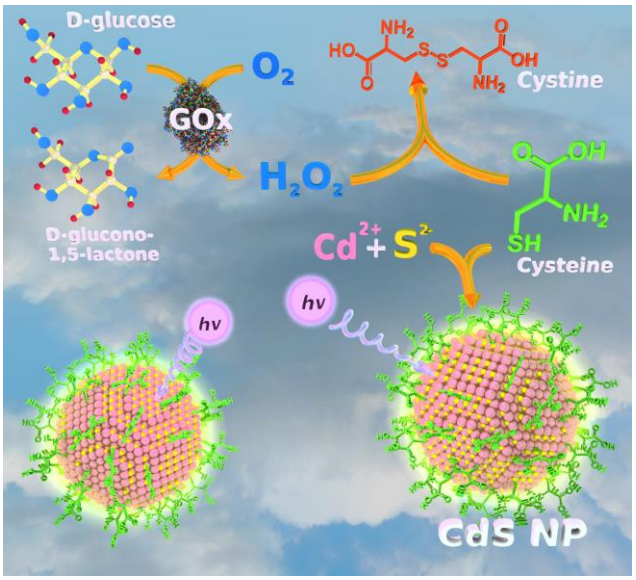

Scheme 2. Fluorometric assay for glucose oxidase activity.

sensitivity that that of the previous published CdS-based fluorogenic assay for GOx [39]. Moreover, this fluorogenic GOx assay is much more sensitive than the colorimetric test for GOx based on CdS NPs [40].

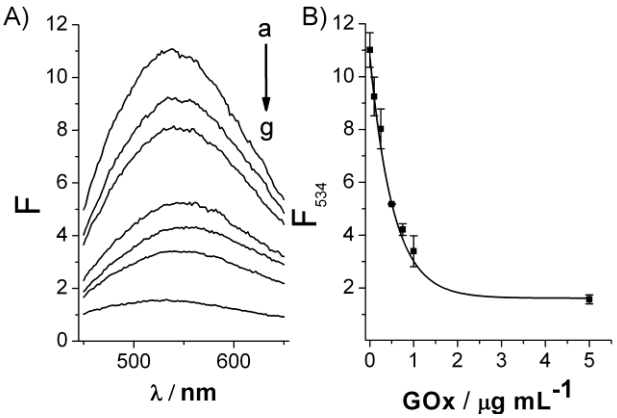

Figure 3. (A) Fluorescence emission spectra of the system containing glucose (1 mM), CSH (0.075 mM), Na_2S (0.1 mM) and $Cd(NO_3)_2$ (1.25 mM) and different concentrations of GOx: a) 0 μg mL^{-1}; b) 0.1 μg mL^{-1}; c) 0.25 μg mL^{-1}; d) 0.5 μg mL^{-1}; e) 0.75 μg mL^{-1}; f) 1 μg mL^{-1}; g) 5 μg mL^{-1}; (B) Calibration curve of GOx obtained using, F_{534}.

We also studied the influence of varying glucose concentrations on the response of our flourogenic assay. Figure 4 shows emission spectra of assay mixtures containing increasing concentrations of glucose and fixed amounts of GOx, CSH, $Cd(NO_3)_2$ and Na_2S. On the basis of the calibration curve in Figure 4.B the LOD of glucose was calculated to be 0.1 mM by UPAC definition [38]. According to the calibration curve (Fig. 4.B) the response to the increasing amounts of glucose was linear within the range from 0 mM to 0.3 mM. Given the fact that the normal level of glucose in human serum published by World Health Organization is < 6.1 mM [41] our assay is even applicable to quantification of glucose in medical laboratories. Therefore, we applied our assay to detection of glucose in human serum employing the standard addition method. In this method several serum sample of the same volume were distributed between different 0.5 mL tubes. The standard known varying amounts of glucose were injected into the samples with human serum. The fluorescence of the samples was measured. The experimental data were plotted with the concentration standards showed in the x-axis and the obtained fluorescence signals in the y-axis of the plot.

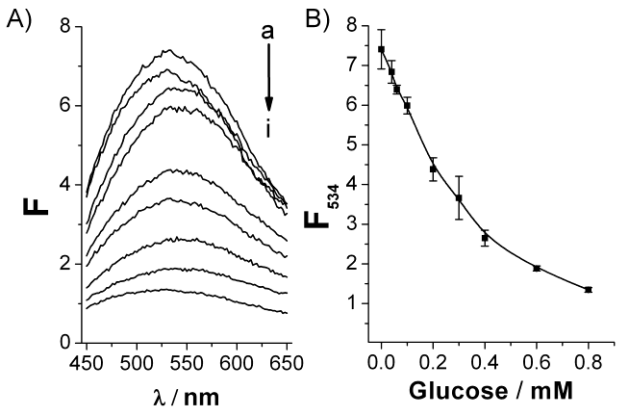

Figure 4. (A) Fluorescence emission spectra of the system containing GOx (5 μg mL^{-1}), CSH (0.075 mM), Na_2S (0.1 mM) and $Cd(NO_3)_2$ (1.25 mM) and different concentrations of glucose: a) 0 mM; b) 0.04 mM; c) 0.06 mM; d) 0.1 mM; e) 0.2 mM; f) 0.3 mM; g) 0.4 mM; h) 0.6 mM; i) 0.8 mM; (B) Calibration curve of glucose obtained using, F_{534}.

The linear regression analysis was performed to calculate the position of the intercept of the calibration line with x-axis, which showed the concentration of glucose in human serum samples (Fig. 5). Taking into consideration all dilutions of the samples, the found concentration of glucose was 6.01 mM. It lies within the limits of normal level of glucose in human serum [41].

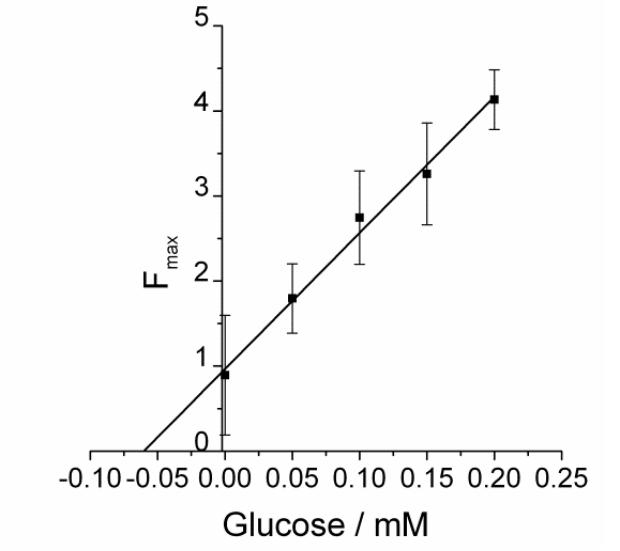

Figure 5. Quantification of glucose in human serum with the method of standard addition. The system contained GOx (5 μg mL^{-1}), CSH (0.075 mM), Na_2S (0.1 mM) and $Cd(NO_3)_2$ (1.25 mM) and various known amounts of added glucose standards.

3.3. Photoelectrochemical detection of glucose

The developed QDs-based PEC system is depicted in Scheme 3. GOx catalyzes oxidation of glucose with oxygen to D-glucono-1,5-lactone and H_2O_2. The former decreases the concentration of CSH modulating the growth of CdS QDs in situ. When the assay solution containing produced CdS QDs is placed over the surface of a SPCE and irradiated with UV light, photons are absorbed by CdS QDs and excite electrons from the occupied valence band (VB) to the empty conduction band (CB) forming electron-hole pairs. CB electrons are transferred from surface of CdS QDs to the electroconductive polymer immobilized on the surface of the SPCE when the positive potential is applied to generate anodic photocurrent. This polymeric electrocatalyst is composed of poly(vinylpyridine) complexed with $Os(bipyridine)_2Cl_2$ (Os–PVP polymer depicted in Fig. S-4 ESM). Holes from VB of CdS QDs are neutralized by the electron donor 1-thioglycerol (TG) which is oxidized to bis(1-thio-2,3 propanediol) at the surface of QDs.

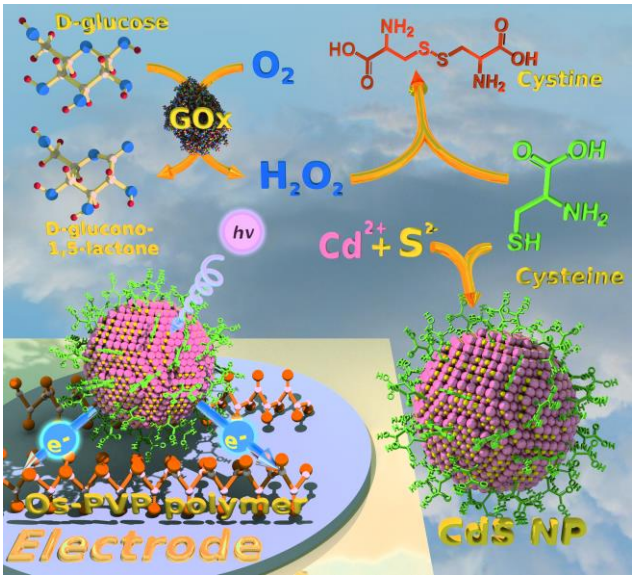

Scheme 3. Electrochemical detection of CdS QDs "wired" by Os-PVP complex to the surface of a SPCE.

In order to photosensitize the surface of SPCE, Os-PVP complex was deposited by cyclic voltammetry (CV) during two cycles in the range from 0 to 0.6 V. After the electrochemical deposition of Os-PVP complex the electrode was washed with water and CV was performed to evaluate the surface coverage of osmium moieties (**Table S-1**). Two redox waves were revealed, confirming that the redox process involves only the central osmium atom (Fig. S-5 ESM). Furthermore, the possible interference from Os-PVP complex with the photocurrent background was assessed at different potentials. The effect of applied potential on the anodic photocurrent is shown in Fig. S-6 (A) ESM. The working potential of 0.3 V *vs.* Ag/AgCl was selected to avoid nonspecific oxidation of TG at the electrode surface. It should be taken into account

that the best ratio of photocurrents registered in the presence and in the absence of CdS QDs (I_{QDs}/I_{Os}) was also achieved at 0.3V *vs.* Ag/AgCl (data not shown)with the signal-to-noise ratio of 3 (S/N = 3). According to the plot representing the effect of different excitation wavelengths on the fluorescence signal (Fig. S-7 ESM), the intensity of the emission peak registered using the excitation wavelength of 365 nm is still higher than 80 % of the maximum emission peak registered using the excitation wavelength of 300 nm. The standard UV illuminator with the maximum output at 365 nm is the most available and inexpensive source of the intense light with the emission peak close to 300 nm therefore it was employed for the photoelectrochemical measurements. All photocurrent responses are presented with the background subtracted at this potential. To estimate the importance of photosensitizing the electrode surface with Os-PVP polymer the control experiment was performed in which non modified SPCE was used for the detection of anodic photocurrent in the presence of CdS QDs and TG in the assay mixture. No significant photocurrent was observed in the absence of Os-PVP polymer on the electrode surface (Fig. S-8 ESM). Thus, Os-PVP polymer is the crucial electrocatalyst mediating the electron transfer of CB electrons from CdS QDs to the SPCE. The photocatalytic oxidation of TG at saturating concentration of 20 mM (Fig. S-9 ESM), which still does not favor its nonspecific electrochemical oxidation, provides the electrons transferred to the surface of the photosensitized SPCEs during quantification of CdS QDs. In the absence of CdS QDs, no significant photocurrent was observed (Figure S-6(B) curve 2).

The influence of the different amounts of glucose on photocurrent is shown in Fig. 6. The decrease in photocurrent is directly related to the increase in the concentration of glucose added to the system. The response shows linearity from 0 to 0.2 mM and saturation starting from 0.4 mM glucose concentration. The LOD was found to be 20 μM (3σ). The average relative standard deviation (RSD) calculated from the glucose calibration plot (obtained using at least three independent SPCEs modified by Os-PVP) was 8%. We also evaluated the response of the system varying the concentration of GOx in the reaction mixture in the presence of 1 mM glucose (Fig. S-10 ESM). According to the calibration curve the LOD was equal to 0.05 μg mL^{-1} (RSD = 4.6%). The control experiments performed in the presence and absence of GOx and glucose showed no significant variation of photocurrent (data no shown).

Comparing with the performance of the fluorogenic method, the PEC system is 5 times more sensitive. Furthermore, the obtained result is also much better than previously published works based on electrochemical detection of glucose, which show worse LODs [42-44].

The standard chromogenic assay for detection of GOx is based on the method previously described in the literature [45]. The chemical interactions employed in the standard commercially available assays:

$$\beta\text{-D-Glucose} + O_2 + H_2O \xrightarrow{GO_x} \text{D-Glucono-1,5-Lactone} + H_2O_2$$

$$H_2O_2 + \text{o-Dianisidine (reduced)} \xrightarrow{HRP} \text{o-Dianisidine (oxidized)}$$

As one can see, this method requires the additional enzyme horseradish peroxidase and very cancerogenic chromogenic dye o-Dianisidine to detect hydrogen peroxide produced by GOx. The commercially available fluorometric kits for detection of GOx (Sigma Aldrich, AbCam) employ fluorogenic substrate of peroxidase 10-acetil-3,7-dihidroxifenoxacina, (AmplexRed®, AbRed®) instead of o-Dianisidine to follow the formation of hydrogen peroxide and require expensive fluorimeters. The dependence of GOx assay on the second enzyme makes the assay prone to errors due to inevitable deactivation of peroxidase even if the components of kits are stored at low temperature.

The photoelectrochemical assay for detection of GOx activity developed by us does require neither expensive fluorogenic dyes nor fluorimeters nor the second enzyme.

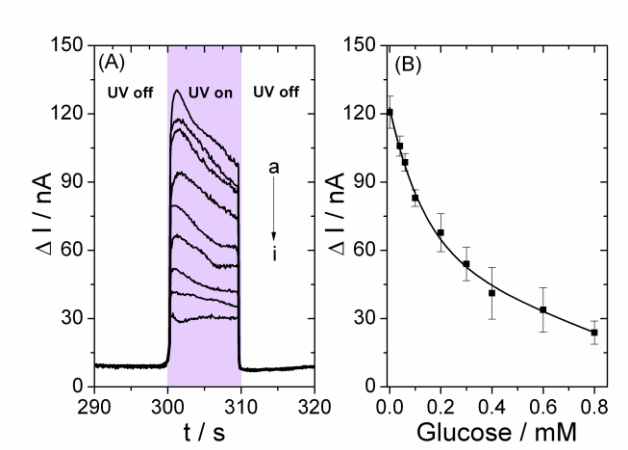

Figure 6. (A) Photocurrent responses of CdS QDs in the system containing GOx (5 μg mL^{-1}), CSH (0.075 mM), TG (20 mM), Na_2S (0.1 mM) and $Cd(NO_3)_2$ (1.25 mM) and different concentrations of glucose: a) 0 mM; b) 0.04 mM; c) 0.06 mM; d) 0.1 mM; e) 0.2 mM; f) 0.3 mM; g) 0.4 mM; h) 0.6 mM; i) 0.8 mM; (B) Calibration curve of GOx obtained at 0.3 V (vs. Ag/AgCl) and 365 nm excitation light.

Finally, the developed sensor was evaluated by the determination of glucose in human serum samples employing the standard addition method. The real samples were not pretreated. As shown in Figure S-6(B) curve 3, electrodes photosensitized with Os-PVP polymer demonstrate a negligible background photocurrent in the presence of human serum samples (around 10 nA) at 0.3V vs. Ag/AgCl. This background current was subtracted from the data of the plot. The known varying amounts of glucose were injected into the samples with human serum. Photocurrents of all samples were measured. The experimental data were plotted with the concentration standards showed in the x-axis and the observed photocurrents in the y-axis of the plot. The intercept of the calibration line with x-axis showing the concentration of glucose in human serum samples was calculated by linear regression (Fig. 7). The found concentration of glucose was 5.06 mM. As reported previously [41], the normal concentration of glucose in human blood is around 5-7 mM. Thus, our device displayed an excellent linear range and RSD values within 10%, showing good sensitivity for detecting glucose.

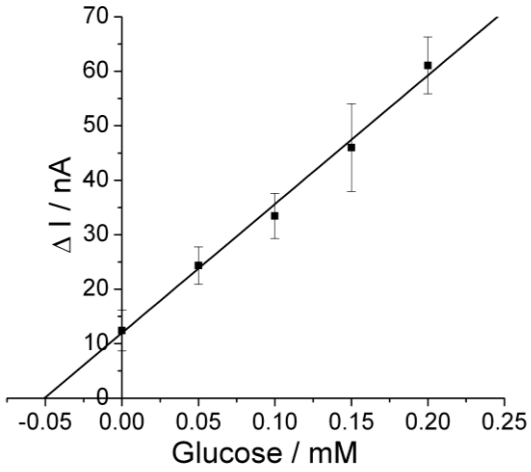

Figure 7. PEC quantification of glucose in human serum with the method of standard addition. The system contained GOx (5 μg mL^{-1}), CSH (0.075 mM), TG (20 mM), Na_2S (0.1 mM) and $Cd(NO_3)_2$ (1.25 mM).

4. Conclusions

The employment of cysteine (CSH) as a capping agent allows for rapid formation of fluorescent CdS QDs in aqueous solutions at room temperature. Hydrogen peroxide (H_2O_2), produced in the course of enzymatic oxidation of D-glucose by glucose oxidase (GOx), oxidizes CSH to cystine (CSSC) modulating the growth of QDs. This biocatalytic process can be applied to the development of simple sensitive fluorometric and photoelectrochemical (PEC) assays for GOx activity in buffered solutions and D-glucose in real samples of human serum using the photocatalytic activity of the resulting QDs. The biocatalytic processes ending up in formation of H_2O_2 are quite abundant in nature. Therefore, we believe that our two model systems potentially can find broad application to

quantify enzymatic activities of many other enzymes generating or consuming H_2O_2.

Acknowledgements

This work was supported by the Spanish Ministry of Economy and Competitiveness (Projects BIO2014-59741-R).

Electronic Supplementary Material: Supplementary material (TEM image of CdS NPs; optimization of CSH concentration; effect of peroxide to preprepared CdS NPs; structure of osmium polymer; control experiments for photoelectrochemical measurements; optimization of 1-thioglycerol concentration; calibration of GOx.) is available in the online version of this article at http://dx.doi.org/10.1007/s12274-***-****-* .

References

[1] Katz, E.; Willner, I. Integrated Nanoparticle–Biomolecule Hybrid Systems: Synthesis, Properties, and Applications. *Angew. Chem., Int. Ed.* **2004**, *43*, 6042-6108.

[2] Liz-Marzán, L. M. Nanometals: Formation and color. *Mater. Today* **2004**, *7*, 26-31.

[3] Li, H.; Xu, D. Silver nanoparticles as labels for applications in bioassays. *TrAC-Trends Anal. Chem.* **2014**, *61*, 67-73.

[4] Omidfar, K.;Khorsand, F.; Darziani Azizi, M. New analytical applications of gold nanoparticles as label in antibody based sensors. *Biosens. Bioelectron.* **2013**, *43*, 336-347.

[5] Mehrabi, M.; Wilson, R. Intercalating gold nanoparticles as universal labels for DNA detection. *Small* **2007**, *3*, 1491-1495.

[6] David, C.;Guillot, N.;Shen, H.;Toury, T.; de la Chapelle, M. L. SERS detection of biomolecules using lithographed nanoparticles towards a reproducible SERS biosensor. *Nanotechnoogyl.* **2010**, *21*, 475501-475507.

[7] Jia, K.;Adam, P. M.;Marks, R. S.; Ionescu, R. E. Fixed Escherichia coli bacterial templates enable the production of sensitive SERS-based gold nanostructures. *Sens. Actuat. B-Chem.* **2015**, *211*, 213-219.

[8] Marks, R. S.; Abdulhalim, I. *Nanomaterials for Water Management: Signal Amplification for Biosensing from Nanostructures*; Pan Stanford: Boca Ratón, 2016.

[9] Jia, K.;Bijeon, J.-L.;Adam, P.-M.; Ionescu, R. E. Large Scale Fabrication of Gold Nano-Structured Substrates Via High Temperature Annealing and Their Direct Use for the LSPR Detection of Atrazine. *Plasmonics* **2013**, *8*, 143–151.

[10] Mayilo, S.;Kloster, M. A.;Wunderlich, M.;Lutich, A.;Klar, T. A.;Nichtl, A.;KÃ¼rzinger, K.;Stefani, F. D.; Feldmann, J. Long-Range Fluorescence Quenching by Gold Nanoparticles in a Sandwich Immunoassay for Cardiac Troponin T. *Nano Lett.* **2009**, *9*, 4558-4563.

[11] Saidi, A.;Mirzaei, M.; Zeinali, S. Using antibody coated gold nanoparticles as fluorescence quenchers for simultaneous determination of aflatoxins (B1, B2) by soft modeling method. *Chemom. Intell. Lab. Syst.* **2013**, *127*, 29-34.

[12] Mirkin, C. A.;Letsinger, R. L.;Mucic, R. C.; Storhoff, J. J. A DNA-based method for rationally assembling nanoparticles into macroscopic materials. *Nature* **1996**, *382*, 607-609.

[13] Pavlov, V.;Xiao, Y.;Shlyahovsky, B.; Willner, I. Aptamer-functionalized Au nanoparticles for the amplified optical detection of thrombin. *J. Am. Chem. Soc.* **2004**, *126*, 11768-11769.

[14] Xiao, Y.;Pavlov, V.;Shlyahovsky, B.; Willner, I. An Os(II)--bisbipyridine--4-picolinic acid complex mediates the biocatalytic growth of au nanoparticles: optical detection of glucose and acetylcholine esterase inhibition. *Chem.-Eur. J.* **2005**, *11*, 2698-2704.

[15] Fanjul-Bolado, P.;Hernandez-Santos, D.;Gonzalez-Garcia, M. B.; Costa-Garcia, A. Alkaline phosphatase-catalyzed silver deposition for electrochemical detection. *Anal. Chem.* **2007**, *79*, 5272-5277.

[16] Shlyahovsky, B.;Katz, E.;Xiao, Y.;Pavlov, V.; Willner, I. Optical and Electrochemical Detection of NADH and of NAD+-Dependent Biocatalyzed Processes by the Catalytic Deposition of Copper on Gold Nanoparticles. *Small* **2005**, *1*, 213-216.

[17] Pavlov, V. Enzymatic Growth of Metal and

Semiconductor Nanoparticles in Bioanalysis. *Part. Part. Syst. Charact.* **2013**, *31*, 36-45.

[18] Merkoçi, A. *Biosensing Using Nanomaterials*; John Wiley & Sons, Inc., 2009.

[19] Garai-Ibabe, G.;Saa, L.; Pavlov, V. Enzymatic product-mediated stabilization of CdS quantum dots produced in situ: application for detection of reduced glutathione, NADPH, and glutathione reductase activity. *Anal. Chem.* **2013**, *85*, 5542-5546.

[20] Saa, L.;Mato, J. M.; Pavlov, V. Assays for methionine gamma-lyase and S-adenosyl-L-homocysteine hydrolase based on enzymatic formation of CdS quantum dots in situ. *Anal. Chem.* **2012**, *84*, 8961-8965.

[21] Chatterjee, A.;Priyam, A.;Das, S. K.; Saha, A. Size tunable synthesis of cysteine-capped CdS nanoparticles by gamma-irradiation. *J. Colloid. Interf. Sci.* **2006**, *294*, 334-342.

[22] Kumar, P.;Kumar, P.;Bharadwaj, L. M.;Paul, A. K.;Sharma, S. C.;Kush, P.; Deep, A. Aqueous Synthesis of l-Cysteine Stabilized Water-Dispersible CdS:Mn Quantum Dots for Biosensing Applications. *BioNanoSci.* **2013**, *3*, 95-101.

[23] Luo, D.;Smith, S. W.; Anderson, B. D. Kinetics and mechanism of the reaction of cysteine and hydrogen peroxide in aqueous solution. *J. Pharm. Sci.* **2005**, *94*, 304-316.

[24] Winterbourn, C. C.; Metodiewa, D. Reactivity of biologically important thiol compounds with superoxide and hydrogen peroxide. *Free Radical Biol. Med.* **1999**, *27*, 322-328.

[25] Barton, J. P.;Packer, J. E.; Sims, R. J. Kinetics of the reaction of hydrogen peroxide with cysteine and cysteamine. *J. Chem. Soc., Perkin Trans. 2* **1973**, 1547-1549.

[26] Bankar, S. B.;Bule, M. V.;Singhal, R. S.; Ananthanarayan, L. Glucose oxidase--an overview. *Biotechnol. Adv.* **2009**, *27*, 489-501.

[27] Zhao, W.-W.;Xu, J.-J.; Chen, H.-Y. Photoelectrochemical bioanalysis: the state of the art. *Chem. Soc. Rev.* **2015**, *44*, 729-741.

[28] Devadoss, A.;Sudhagar, P.;Terashima, C.;Nakata, K.; Fujishima, A. Photoelectrochemical biosensors: New insights into promising photoelectrodes and signal amplification strategies. *J. Photochem. Photobiol., C* **2015**, *24*, 43-63.

[29] Yue, Z.;Lisdat, F.;Parak, W. J.;Hickey, S. G.;Tu, L.;Sabir, N.;Dorfs, D.; Bigall, N. C. Quantum-Dot-Based Photoelectrochemical Sensors for Chemical and Biological Detection. *ACS Appl. Mater. Interfaces* **2013**, *5*, 2800-2814.

[30] Zhou, H.;Liu, J.; Zhang, S. Quantum dot-based photoelectric conversion for biosensing applications. *TrAC-Trends Anal. Chem* **2015**, *67*, 56-73.

[31] Zhao, W.-W.;Wang, J.;Zhu, Y.-C.;Xu, J.-J.; Chen, H.-Y. Quantum Dots: Electrochemiluminescent and Photoelectrochemical Bioanalysis. *Anal. Chem.* **2015**, *87*, 9520-9531.

[32] Walcarius, A. Electrocatalysis, sensors and biosensors in analytical chemistry based on ordered mesoporous and macroporous carbon-modified electrodes. *TrAC-Trends Anal. Chem.* **2012**, *38*, 79-97.

[33] Long, Y.-T.;Kong, C.;Li, D.-W.;Li, Y.;Chowdhury, S.; Tian, H. Ultrasensitive Determination of Cysteine Based on the Photocurrent of Nafion-Functionalized CdS–MV Quantum Dots on an ITO Electrode. *Small* **2011**, *7*, 1624-1628.

[34] Zhao, W.-W.;Ma, Z.-Y.;Yan, D.-Y.;Xu, J.-J.; Chen, H.-Y. In Situ Enzymatic Ascorbic Acid Production as Electron Donor for CdS Quantum Dots Equipped TiO2 Nanotubes: A General and Efficient Approach for New Photoelectrochemical Immunoassay. *Anal. Chem.* **2012**, *84*, 10518-10521.

[35] Zhou, H.; Liu, J.; Zhang, S. Quantum dot-based photoelectric conversion for biosensing applications. *TrAC-Trends Anal. Chem.* **2015**, *67*, 56-73.

[36] Iyer, R.; Pavlov, V.;Katakis, I.; Bachas, L. G. Amperometric Sensing at High Temperature with a "Wired" Thermostable Glucose-6-phosphate Dehydrogenase from Aquifex aeolicus. *Anal. Chem.* **2003**, *75*, 3898-3901.

[37] Vreeke, M. S.;Yong, K. T.; Heller, A. A Thermostable Hydrogen Peroxide Sensor Based on "Wiring" of Soybean Peroxidase. *Anal. Chem.* **1995**, *67*, 4247-4249.

[38] McNaught, A. D.; Wilkinson, A. IUPAC Compendium of

Chemical Terminology. . In *Gold Book*; Oxford, UK, 1997.

[39] Saa, L.; Pavlov, V. Enzymatic growth of quantum dots: applications to probe glucose oxidase and horseradish peroxidase and sense glucose. *Small* **2012**, *8*, 3449-3455.

[40] Grinyte, R.;Garai-Ibabe, G.;Saa, L.; Pavlov, V. Application of photocatalytic cadmium sulfide nanoparticles to detection of enzymatic activities of glucose oxidase and glutathione reductase using oxidation of 3,3',5,5'-tetramethylbenzidine. *Anal. Chim. Acta* **2015**, *881*, 131-138.

[41] Rodriguez, B. L.;Abbott, R. D.;Fujimoto, W.;Waitzfelder, B.;Chen, R.;Masaki, K.;Schatz, I.;Petrovitch, H.;Ross, W.;Yano, K.;Blanchette, P. L.; Curb, J. D. The American Diabetes Association and World Health Organization Classifications for Diabetes. In *Their impact on diabetes prevalence and total and cardiovascular disease mortality in elderly Japanese-American men*, 2002; pp 951-955.

[42] Li, W.;Qian, D.;Wang, Q.;Li, Y.;Bao, N.;Gu, H.; Yu, C. Fully-drawn origami paper analytical device for electrochemical detection of glucose. *Sens. Actuat. B-Chem.* **2016**, *231*, 230-238.

[43] Li, L.;Liang, B.;Li, F.;Shi, J.;Mascini, M.;Lang, Q.; Liu, A. Co-immobilization of glucose oxidase and xylose dehydrogenase displayed whole cell on multiwalled carbon nanotube nanocomposite films modified electrode for simultaneous voltammetric detection of d-glucose and d-xylose. *Biosens. Bioelectron.* **2013**, *42*, 156-162.

[44] Tanne, J.;Schäfer, D.;Khalid, W.;Parak, W. J.; Lisdat, F. Light-Controlled Bioelectrochemical Sensor Based on CdSe/ZnS Quantum Dots. *Anal. Chem.* **2011**, *83*, 7778-7785.

[45] Bergmeyer, H. U., Gawehn, K., Grassl, M. *Methods of Enzymatic Analysis*; Academic Press: New York, 1974.

.

Electronic Supplementary Material

Modulation of Growth of Cysteine-capped Cadmium Sulphide Quantum Dots with Enzymatically produced Hydrogen Peroxide

Ruta Grinyte[1], Javier Barroso[1], Laura Saa[1], Valeri Pavlov[1] ✉

[1] Biosensing Unit, CIC BiomaGUNE, Parque Tecnológico de San Sebastian, Paseo Miramón 182, Donostia-San Sebastián, 20009 Spain

Supporting information to DOI 10.1007/s12274-****-****-* (automatically inserted by the publisher)

List of Electronic Supplementary Material:

Address correspondence to Valeri Pavlov, vpavlov@cicbiomagune.es

1. Optical method

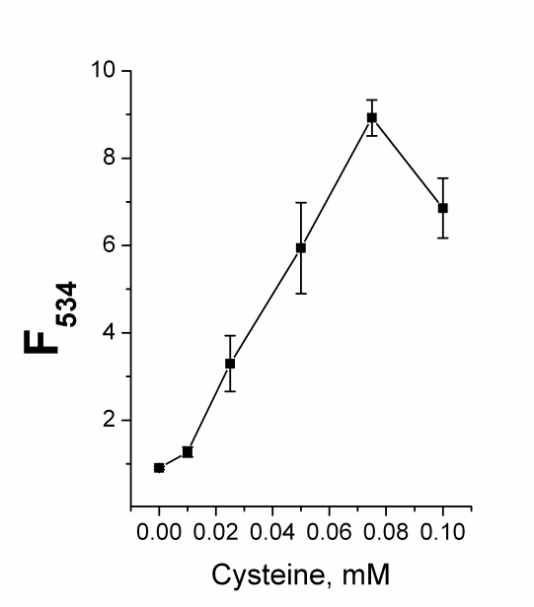

Fig. S-1 Effect of cysteine concentration on fluorescence intensity in the reaction mixture composed of Na_2S 0.1 mM and $Cd(NO_3)_2$ 1.25 mM. Incubation time 5 min, λ_{exc} = 300 nm.

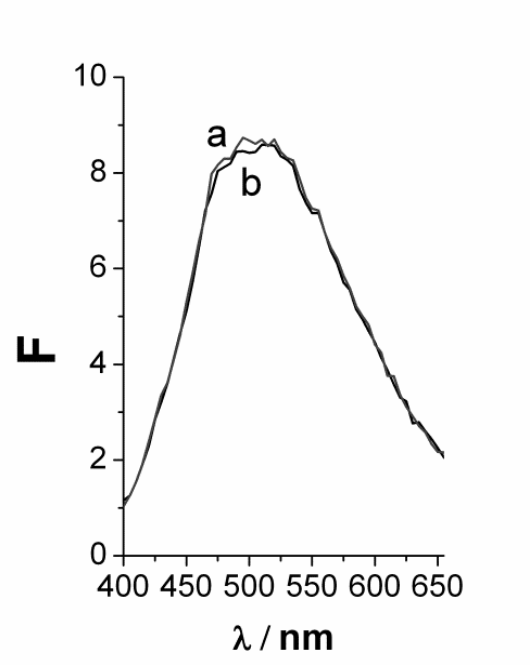

Fig. S-2 The system containing cysteine-stabilized CdS QDs before addition of H_2O_2 (curve a) and after addition of 0.1 mM of H_2O_2 (curve b). Incubation time 5 min, λ_{exc} = 300 nm.

2. TEM images of CdS QDs and size distribution

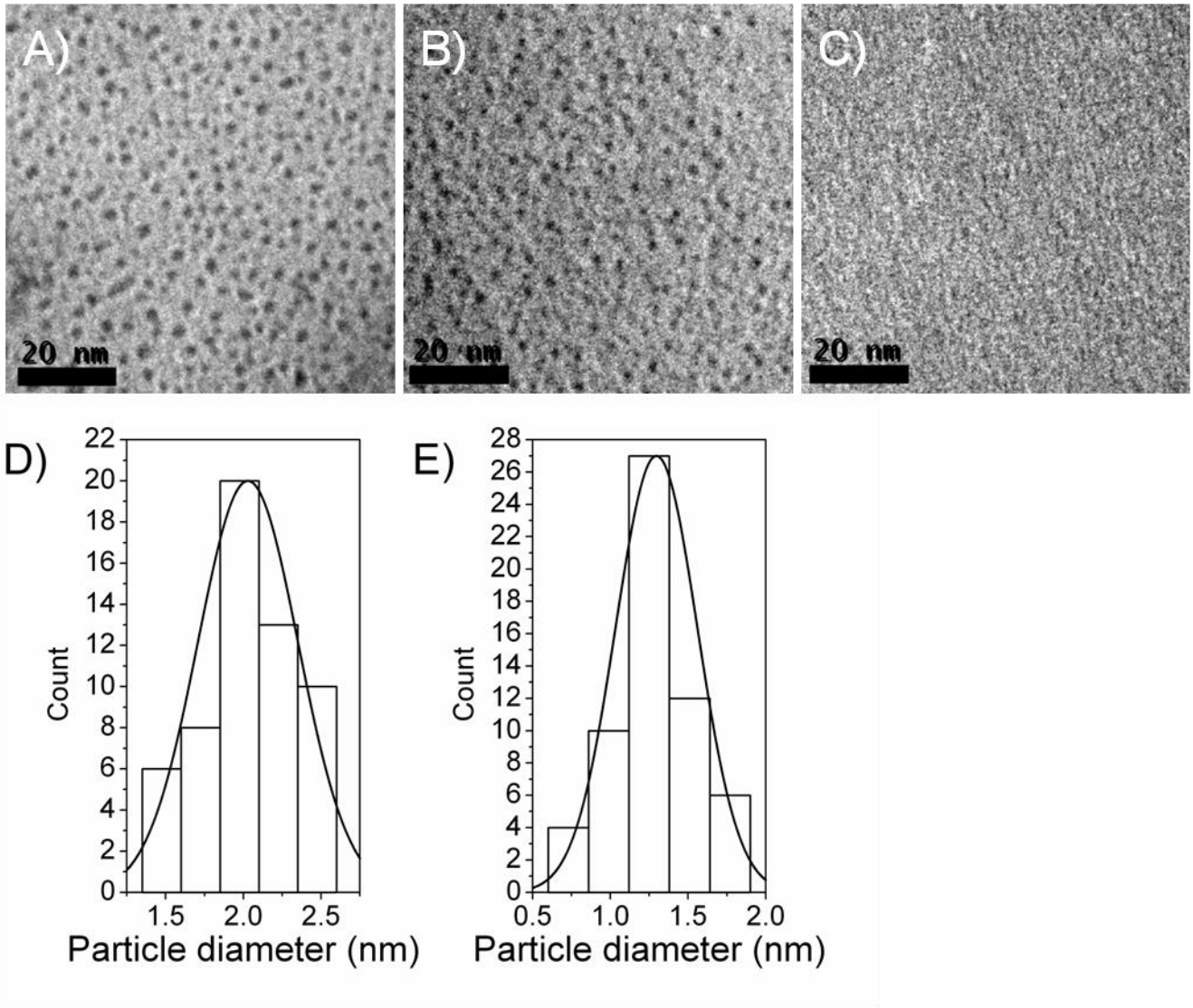

Fig. S-3 TEM images of cysteine stabilized CdS QDs in the presence of (A) 0 mM of H_2O_2 (B) 0.03 mM of H_2O_2 (C) 0.3 mM of H_2O_2; Size distribution of cysteine stabilized CdS QDs in the presence of (D) 0 mM of H_2O_2 (E) 0.03 mM of H_2O_2.

3.- Structure of osmium polymer

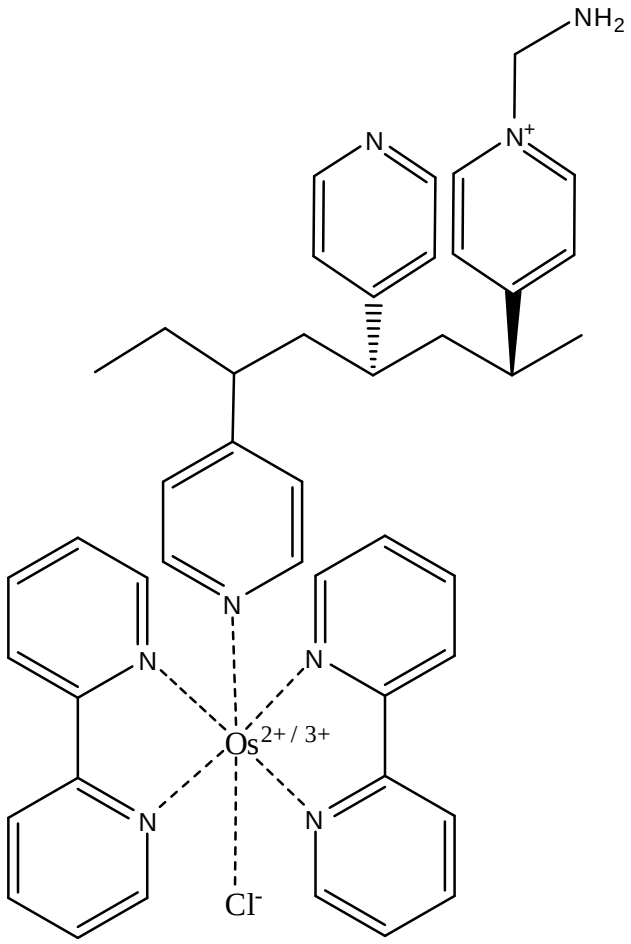

Fig. S-4. 2D structure of poly(vinypyridine) complexed with $Os(bipyridine)_2Cl_2$ (Os-PVP complex).

The polymer was synthesized according to the procedure previously published elsewhere (Katakis I., Ye L., Heller A., 1994. J. Am. Chem. Soc. 116, 3617-3618).

4. Electrochemical characterization of SPCEs

Surface coverage (Γ) of electroactive species was determined by cyclic voltammetry (CV) calculating the charge under the areas of peaks depicted in Fig. S5.

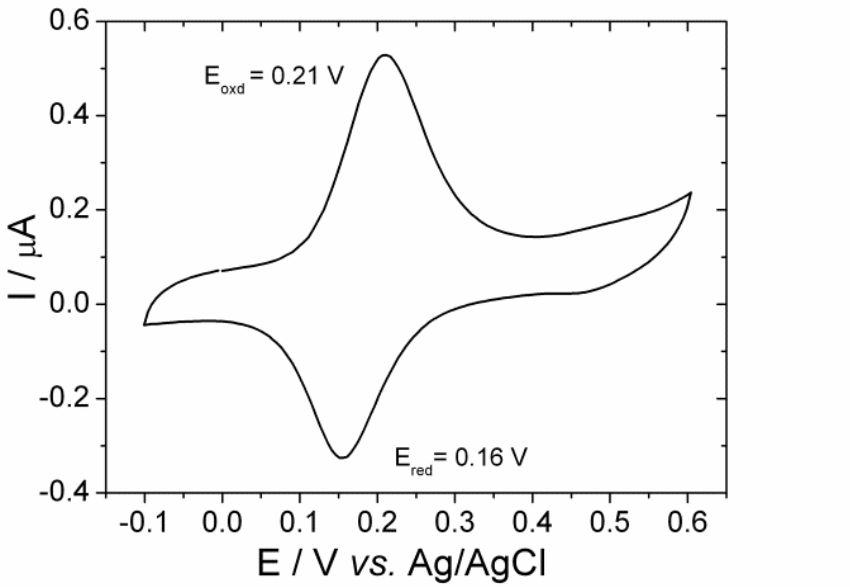

Fig. S-5 Cyclic voltammograms of screen-pirnted carbon electrode (SPCE) modified by Os-PVP complex. Scan rate of 50 mV s^{-1}.

Taking into account the number of exchanged electrons per redox molecule and the Faraday´s constant, the surface concentration was calculated. The peak intensity, I_p, is a function of scan rate υ, charge diffusion coefficient D_0, number of exchanged electrons n, surface concentration of redox active species C_0^*, surface coverage Γ, electrode surface area A, temperature T, Faraday´s constant F and gas constant R according to the equation:

$$I_p = n^2F^2\Gamma A\upsilon(4RT)^{-1}$$

The Randles-Sevčik equation for quasi-reversible electron transfer processes was employed to determine the active electrode area, as follows:

$$I_p = (2.65 * 10^5)n^{3/2}ACD^{1/2}\upsilon^{1/2}$$

where n is the number of electrons participating in the redox process, A is the active electrode area, D is the diffusion coefficient, C is the concentration of probe molecule and υ is the scan rate. The CV were performed in potasium ferricyanide (2mM). The calculations of active area (A) were carried out employing the value of D mentioned by Kadara et al., 2009. The electrochemically active area was 0.099 cm^2. The surface coverage is shown in Table S-1 for three independent screen-printed carbon electrodes (SPCEs) modified by Os-PVP complex. The average coverage was found to be 10.9 ± 1.4 nmol cm^{-2}.

Table S-1 Surface coverage (Γ / nmol cm^{-2}) of three independent screen-printed carbon electrodes.

Electrode	Γ / nmol cm^{-2}
1	**11.2**
2	**12.1**
3	**9.4**

References

1. Prodromidis M.I., Florou A.B., Tzouwara-Karayanni S.M., Karayannis M.I., 2000. Electroanal. 12, 1498-1501.
2. Gao Z., Binyamin G., Kim H.H., Barton S.C., Zhang Y., Heller A., 2002. Angew. Chem. Int. Ed. 41, 810-813.
3. Kadara R.O., Jenkinson N., Banks C.E., 2009. Sensor Actuat B-Chem. 138,556–562.

5. Photoelectrochemical control

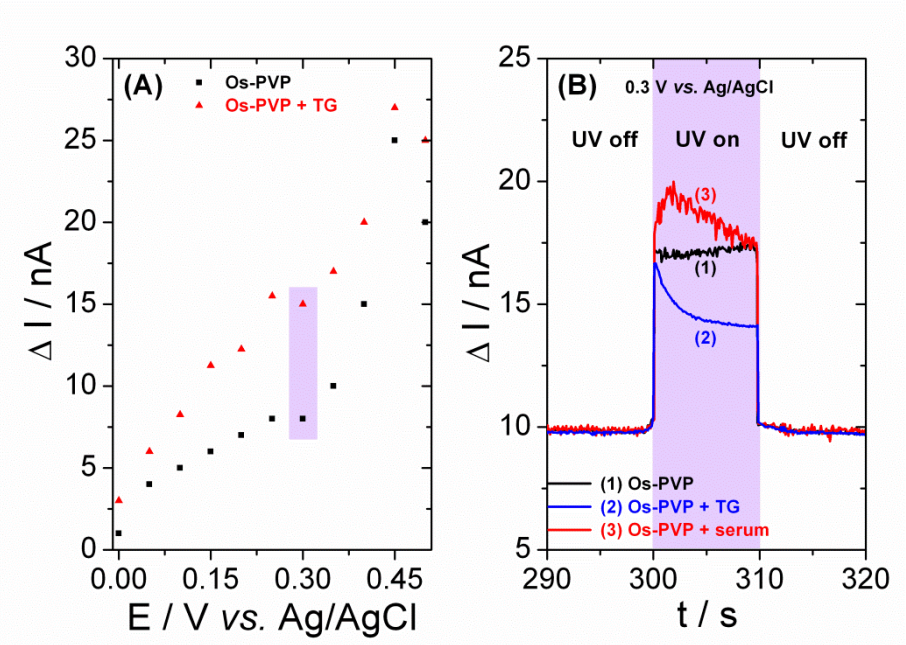

Fig. S-6 (A) Variation in the photocurrent for the modified SPCE sensitized by conductive OS-PVP complex in the presence and in the absence of 1-thioglycerol (TG) in the potential range between from 0 to 0.5 V vs. Ag/AgCl; (B) Photocurrent background responses in the absence of CdS QDs on the SPCE containing (1) only Os-PVP complex; (2) Os-PVP complex, 1-thioglycerol (TG) 20 mM and (3) Os-PVP complex, human serum.

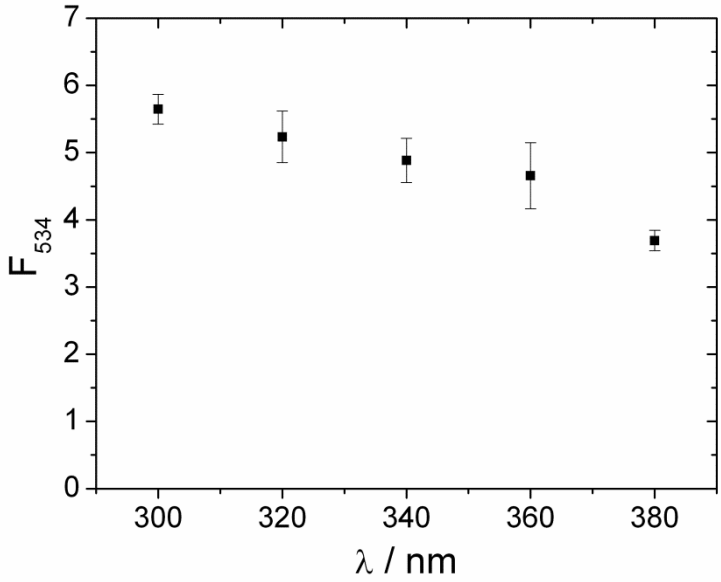

Fig. S-7 The plot showing the dependence of the emission light intensity, registered in the reaction mixture containing CdS QDs, on the wavelength of the excitation light.

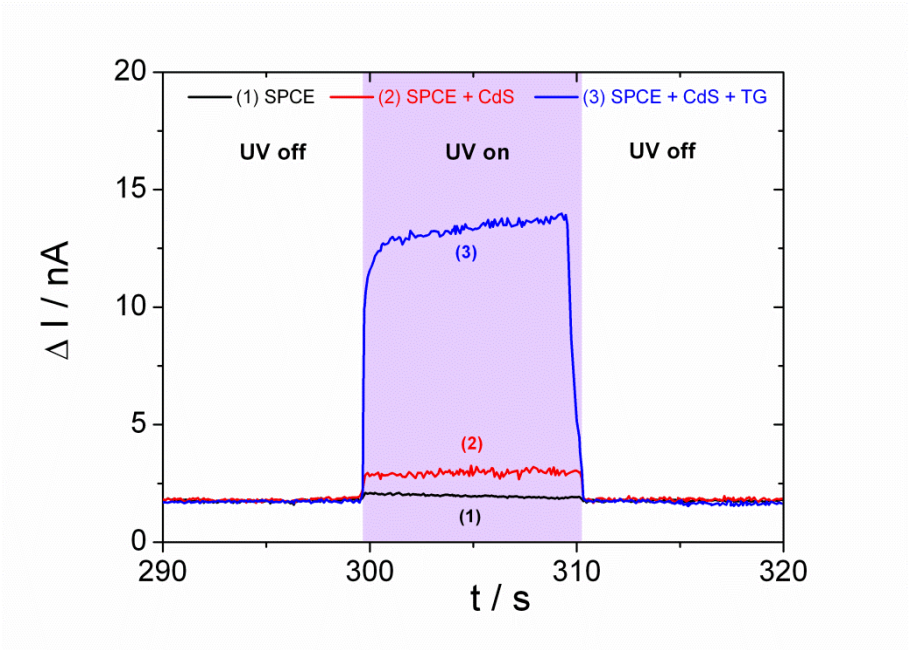

Fig. S-8 Photocurrent background responses in the absence of Os-PVP complex for (1) only SPCE; (2) SPCE and CdS QDs and (3) SPCE, CdS QDs and 1-thioglycerol (TG) 20 mM.

6. Optimization of 1-thioglycerol concentration

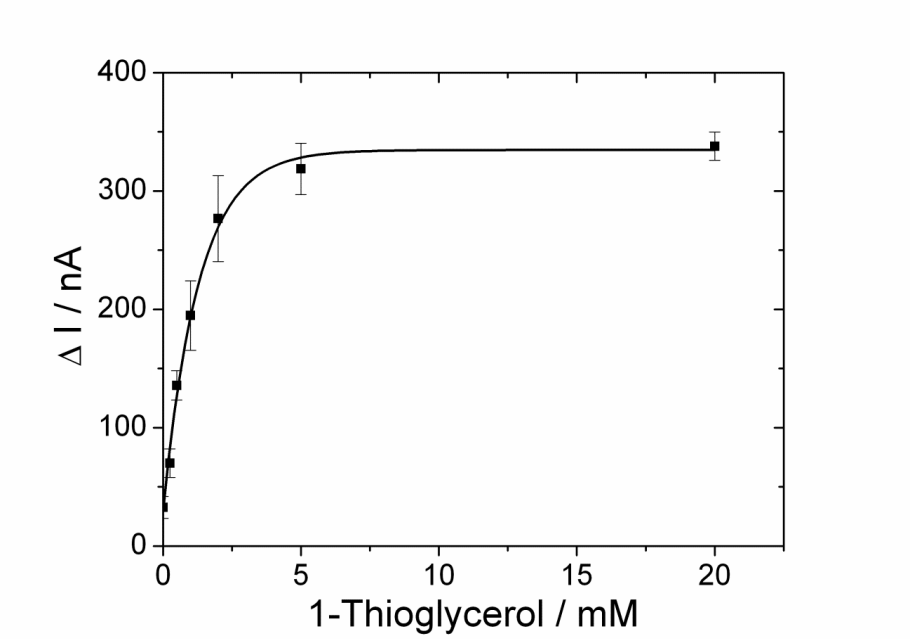

Figure S-9 Effect of the increasing 1-thioglycerol concentrations (TG) on photocurrent observed in the presence of CdS QDs at 0.3 V (*vs.* Ag/AgCl) and 365 nm excitation light. Concentrations of TG: a) 0 mM; b) 0.25 mM; c) 0.5 mM; d) 1 mM; e) 2 mM; f) 5 mM; g) 20 mM. The the system contains $Cd(NO_3)_2$ (1.25 mM), Na_2S (0.1 mM) and cysteine (0.075 mM). The average relative standard deviation (RSD) calculated from the plot (obtained using at least three independent SPCEs modified by Os-PVP) was 9.75 %.

7. Optimization of glucose oxidase concentration for photoelectrochemical measurements

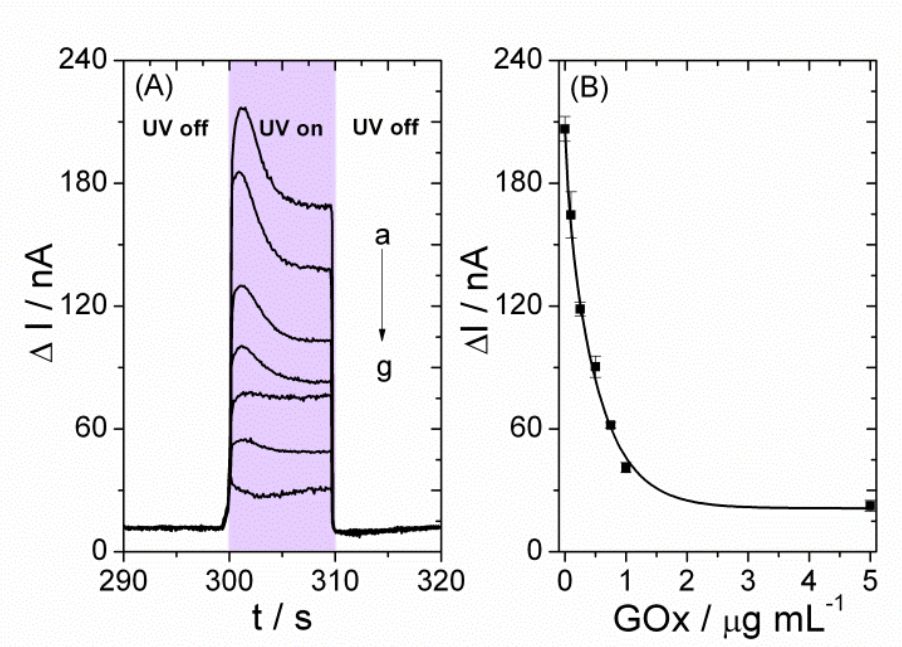

Fig. S-10 (A) Photocurrent responses of the system containing glucose (1 mM), cysteine (0.075 mM), 1-thioglycerol (TG) 20 mM, Na_2S (0.1 mM) and $Cd(NO_3)_2$ (1.25 mM) and different concentrations of GOx: a) 0 μg mL^{-1}; b) 0.1 μg mL^{-1}; c) 0.25 μg mL^{-1}; d) 0.5 μg mL^{-1}; e) 0.75 μg mL^{-1}; f) 1 μg mL^{-1}; g) 5 μg mL^{-1}; (B) Calibration curve of GOx obtained at 0.3 V (vs. Ag/AgCl) and 365 nm excitation light.

TABLE OF CONTENTS (TOC)

Modulation of Growth of Cysteine-capped Cadmium Sulphide Quantum Dots with Enzymatically produced Hydrogen Peroxide

Ruta Grinyte, Javier Barroso, Laura Saa, Valeri Pavlov*

Biofunctional Nanomaterials Unit, CIC BiomaGUNE, Parque Tecnológico de San Sebastian, Paseo Miramón 182, Donostia-San Sebastián, 20009 Spain

Page Numbers. The font is ArialMT 16 (automatically inserted by the publisher)

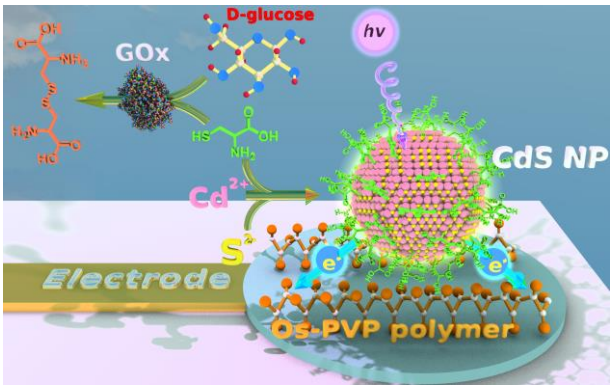

Enzymatically produced hydrogen peroxide oxidizes cysteine modulating the growth of quantum dots. This system allows quantification of glucose oxidase and glucose in human serum, using fluorescence spectroscopy and photoelectrochemical analysis.

Nano Res
DOI (automatically inserted by the publisher)
Review Article/Research Article **Please choose one**

Modulation of Growth of Cysteine-capped Cadmium Sulphide Quantum Dots with Enzymatically produced Hydrogen Peroxide

Ruta Grinyte[1], Javier Barroso[1], Laura Saa[1], Valeri Pavlov[1] ✉

[1] Biosensing Unit, CIC BiomaGUNE, Parque Tecnológico de San Sebastian, Paseo Miramón 182, Donostia-San Sebastián, 20009 Spain

Received: day month year / Revised: day month year / Accepted: day month year (automatically inserted by the publisher)

ABSTRACT

Cysteine (CSH) readily stabilizes CdS quantum dots (QDs) growing in aqueous buffered solutions. Oxidation of CSH by hydrogen peroxide (H_2O_2) at room temperature yields cystine (CSSC) which does not stabilize CdS QDs so efficiently as CSH does. Here we demonstrate that such oxidation causes the decrease in the rate of the formation of CSH - capped CdS QDs from Cd^{2+} and S^{2-} ions. For the first time, we combined the oxidation of CSH with biocatalytic oxidation of D-glucose catalyzed by glucose oxidase (GOx) leading to the buildup of hydrogen peroxide in the reaction mixture. Enzymatically modulated growth of CdS QDs in situ was monitored by two techniques: fluorescence spectroscopy and photoelectrochemical (PEC) analysis. This system allowed quantification of GOx and glucose in human serum.

KEYWORDS

quantum dots, photoelectrochemistry, enzyme, fluorescence, hydrogen peroxide

1. Instruction

The unstoppable development of nanotechnology during the last decades has allowed for the fabrication of new materials and design of novel biosensing methods. One of the valuable tools employed in biosensing are inorganic nanoparticles (NPs). NPs of noble metals like gold and silver exhibit high extinction coefficients due to surface plasma resonance [1]. The optical properties of metal NPs depend on their shape and size [2]. Traditionally metal NPs were used in bioanalysis as labels in affinity assays [3-5]; enhancers of raman scattering [6-9]; quenchers of fluorescence [10, 11] and scaffolds for assembling of biorecognition elements [12, 13]. Metal NPs can be produced in situ with

Address correspondence to Valeri Pavlov, vpavlov@cicbiomagune.es

biocatalytic processes catalyzed by different enzymes, for instance, glucose oxidase (GOx), alkaline phosphatase (ALP), and alcohol dehydrogenase (AlcDH) [14-16]. Metal NPs generated in situ by enzymes usually are not fluorescence and hardly demonstrate photocatalitic activities. This feature limits their employment in bioassays.

NPs composed of semiconductor materials demonstrate quantum effects and can be photoexcited emitting photons during the relaxation process. Therefore, those particles are referred to in the literature as quantum dots (QDs). They find broad application in nanotechnology, diagnostics and therapy [1, 17-20]. The energy of the emitted photons and consequently the intensity and the wavelength of the observed fluorescence depend on the nature and the shape of QDs, the environment and capping agents (stabilizers).

Cysteine (CSH), which carries thiol functional group for binding at CdS interface and hydrophilic amino and carboxylic groups, is an efficient stabilizer of CdS NPs [21, 22]. On the other hand, CSH can be easily oxidized to form a dimer containing disulfide bridge between two CSHs, known as cystine (CSSC). Oxidation of CSH with hydrogen peroxide (H_2O_2) in aqueous buffers can be described by the two-step nucleophilic reaction model [23-25]. This process is initiated by rate-determining nucleophilic attack of thiolate anion (CS^-) on unionized H_2O_2 to generate sulfenic acid (CSOH) as an intermediate product (Equation 1). The latter interacts with CS^- ions to yield CSSC as shown in equation 2.

$$CS^- + H_2O_2 \rightarrow CSOH + HO^- \quad (1)$$

$$CSOH + CS^- \rightarrow CSSC + HO^- \quad (2)$$

For the first time, we combined this reaction with biocatalytic oxidation of D-glucose (glucose) catalyzed by GOx leading to the buildup of H_2O_2 in the reaction mixture. GOx is the protein composed of two identical 80 kDa subunits containing two bound FAD coenzymes. Chemical, pharmaceutical, food, beverage, clinical chemistry, biotechnology and other industries broadly employ GOx [26]. The determination of GOx enzymatic activity is quite important in industry. The standard assay for GOx activity relies on the reaction mixture containing the additional enzyme horseradish peroxidase (HRP) that is used for detection of H_2O_2 produced by GOx (enzymatic assay of GOx from Sigma-Aldrich).

In the present work we demonstrate that the oxidation of the stabilizing agent CSH by H_2O_2 produced by GOx causes the decrease in the rate of the formation of CSH-capped CdS QDs from Cd^{2+} and S^{2-} ions. This process allows relating the enzymatic activity of GOx and glucose concentration with amount of CdS QDs produced in situ which defines the emission spectrum of the assay mixture followed by the fluorescence spectroscopy, the extremely sensitive laboratory technique for detection of the fluorescence readout signal.

We also used the powerful alternative to fluorometry, the photoelectrochemical (PEC) analysis [27, 28]. PEC sensors are becoming a promising low cost approach for the detection of light responsive chemical and biochemical molecules [29-31]. The process of PEC detection converts luminous energy into electrochemical energy at the surface of the electrode, generating electrical readout signal. The photocurrent intensity is defined by the characteristics of excitation light, applied potential and the rate of the electron transfer between the electron surface and QDs. A number of electrocatalysts have been applied to facilitate the electron transfer to the electrode surface in PEC analysis, such as microporous carbon including carbon nanotubes and grapheme [32], small organic molecules like methyl viologen immobilized on polymeric nafion matrix [33],

semiconductor metal oxides like TiO_2 [34]. Usually electrocatalysts were immobilized on expensive gold and indium tin oxide (ITO) electrodes using anchoring thiol and silane groups [35]. Screen-printed carbon electrodes (SPCE) are significantly cheaper but their modification with electrocatalysts is quite difficult due to the absence of anchoring functional groups on the surface of the carbon material of the working electrode. In the present work we employ the complex of poly(vinylpyridine) with $Os(bipyridine)_2Cl_2$ (Os-PVP complex) as the electrocatalyst to facilitate the electron exchange. Previously, the redox polymer of this structure was applied to wire redox enzymes, for instance, glucose-6-phosphate dehydrogenase [36] and HRP [37].

In this article we present a new strategy for detection of enzymatic activities using the fluorescent spectroscopy and PEC. We offer a quite universal bioanalytical platform relying on the enzymatically modulated growth of CdS QDs in situ followed by two techniques which finally will be applicable to the range of detection systems spanning from optical laboratory equipment to low power mobile fast point of care (POC) analytical systems.

2. Experimental

Materials. Sodium sulfide (Na_2S), cadmium nitrate $Cd(NO_3)_2$, glucose oxidase type VII from Aspergillus niger and other chemicals were purchased from Sigma Aldrich. Anhydrous ß-D-glucose and hydrogen peroxide (30% v/v) were purchased from Panreac.

Characterisation. *Spectroscopy.* Transmission electron miscroscopy (TEM) images were collected with a JEOL JEM 2100F operating at 120 kV.

Optical methods. Fluorescence measurements were performed on a Varioskan Flash microplate reader (Thermo Scientific) using black microwell plates at room temperature. The system was controlled by SkanIt Software 2.4.3. RE for Varioskan Flash.

Photoelectrochemistry. All electrochemical experiments were conducted in the Autolab Electrochemical Workstation (Model: PGSTAT302N, Metrohm Autolab, The Netherlands) equipped with NOVA 1.10 software. Disposable screen-printed carbon electrodes (SCPEs) were purchased from DropSens (model DRP-110, 4 mm diameter). Electrical contact to workstation was done with a special boxed connector supplied by DropSens. The illumination source was a compact UV illuminator (UVP, Analytik Jena AG). All PECs were performed at room temperature. All the potentials reported in our work were against Ag/AgCl. Unless mentioned otherwise, all experimental results presented here are averaged from three independent measurements (n = 3).

Methods CdS QD-mediated determination of H_2O_2. Different concentrations of H_2O_2 were incubated with 0.075 mM of CSH in citrate-phosphate buffer (pH 7.5) for 40 min at room temperature. After that, Na_2S (10 µL , 1 mM) and $Cd(NO_3)_2$ (2.5 µL , 50 mM) were added to the samples (87.5 µL). The emission spectra of the resulting suspensions were recorded after 5 min at λ_{exc} = 300 nm.

GOx assay. Varying amounts of glucose were incubated with different amounts of GOx in citrate-phosphate buffer (pH 7.5) for 40 min at room temperature, in the presence of CSH (0.075 mM). After that, Na_2S (10 µL, 1 mM) and $Cd(NO_3)_2$ (2.5 µL, 50 mM) were added to the samples (87.5 µL). The emission spectra of the resulting CdS QDs were recorded after 5 min at λ_{exc} = 300 nm.

Quantification of glucose in human serum. Quantification of glucose in human serum was performed by the standard edition method. Samples of pooled human serum (Sigma-Aldrich) were spiked with known different concentrations of glucose and the glucose concentration of the

mixtures was determined. The dilution factor of plasma in the assay was 1:100.

Photoelectrochemical detection. SPCEs were initially pretreated electrochemically by cyclic voltammetry (CV) at a potential range of 0 – 0.8 V in citrate-phosphate buffer (pH 7.5). Subsequently, a 40 μL drop of Os-PVP complex (1.375 mg mL^{-1}) was placed on the SPEs and deposited by CV scanning (2 cycles, 50 mV s^{-1}). Later, SPCEs were rinsed out with ultrapure water and dried under argon atmosphere. Finally, a 40 μL of samples were dropped on the SPCE and PEC measurements were carried out with UV illuminator at 365 nm and a controlled potential of 0.3 V. The dependence of photocurrent on time was measured at 5 minutes during 10 seconds. 1-thioglycerol (TG) was added to the samples to amplify the signal.

3. Results and discussion

3.1. CdS QD-mediated determination of H_2O_2 and optimization of the system

The ability of CSH to stabilize CdS QDs was studied. Cadmium nitrate ($Cd(NO_3)_2$) was interacted with sodium sulfide (Na_2S), in citrate phosphate buffer (pH 7.5) in the presence of CSH or CSSC, which is the oxidized form of CSH. The formation of fluorescent CdS QDs was followed by fluorescence spectroscopy. As one can see in Fig. 1 reaction mixture containing CSH, Cd^{2+} and S^{2-} ions demonstrated high emission peak (curve a). No significant fluorescence was observed in the presence of CSSC (curve b) or without any CSH and CSSC (curve c). This finding proves that CSSC does not stabilize fluorescent QDs so efficiently as CSH (Figure 1, curve b). In order to increase the yield of CSH-stabilized CdS NPs the effect of CSH concentration on fluorescence spectrum of the reaction mixtures containing Cd^{2+} and S^{2-} ions was investigated. According to Fig. S-1 Electronic Supplementary Material (ESM) optimum concentration of CSH was 0.075 mM, which was used in all subsequent experiments.

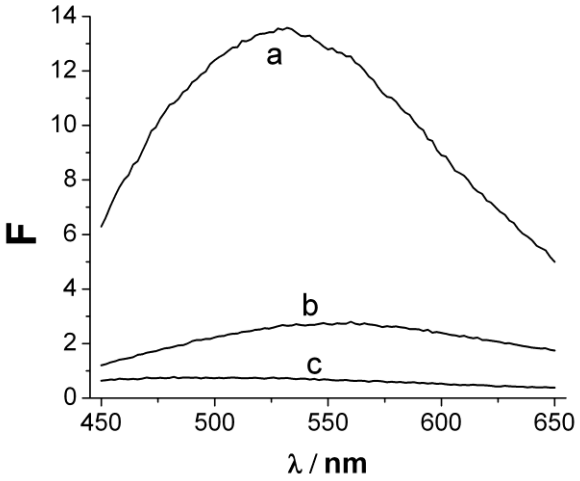

Figure 1. Fluorescence emission spectra of the system containing (a) CSH (0.5 mM), Na_2S (0.1 mM), $Cd(NO_3)_2$ (1.25 mM); (b) CSSC (0.5 mM), Na_2S (0.1 mM), $Cd(NO_3)_2$ (1.25 mM); (c) only Na_2S (0.1 mM) and $Cd(NO_3)_2$ (1.25 mM)

Thus, CSH is able to stabilize CdS NPs formed in situ from S^{2-} and Cd^{2+} ions in aqueous solutions within the incubation time of 5 min at room temperature (Scheme 1). The previously published procedures for the synthesis of CSH-stabilized CdS QDs required much longer incubation times (over 1 hour) and very harsh experimental conditions like high temperatures (over 80 °C) [22] or irradiation with γ-rays [21]. The process of CdS QDs formation under physiological conditions, optimized by us, was very rapid and compatible with natural biochemical pathways leading to oxidation of CSH for modulation of QDs' growth.

It was found out that the treatment of CSH with varying concentrations of H_2O_2 leads to the decrease in the rate of formation of CdS NPs due to

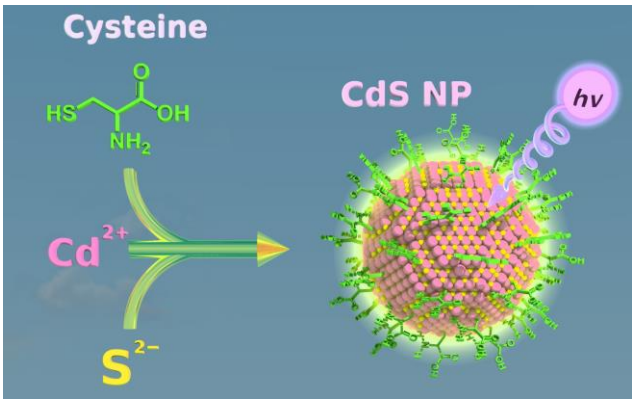

Scheme 1. Modulation of CdS QDs growth with cysteine.

oxidation of CSH into CSSC. As one can see in Fig. 2, the decrease in the fluorescence signal was directly related to the quantity of the H_2O_2 in the reaction mixture. Calibration curve shown in Figure 2 inset demonstrated linearity from 0.0 to 0.045 mM and saturation starting from 0.15 mM H_2O_2 concentration. In accordance with the calibration curve the limit of H_2O_2 detection (LOD) was calculated to be 12.6 μM by UPAC definition [38]. This LOD is 4 times lower than that of the reported most relevant fluorogenic assay for detection of H_2O_2 using the enzymatic growth of CdS NPs [39]. It is important to note that after addition of H_2O_2 (0.1 mM) to the pre-prepared CdS NPs stabilized with CSH no changes in the emission spectra of CdS NPs were noticed (Fig. S-2, curve b ESM). So, the decrease in the fluorescence was not caused by the possible quenching effect of H_2O_2. Transmission electron microscopy (TEM) was applied to confirm the existence of CSH stabilized CdS QDs in the reaction mixture at three different concentration of H_2O_2 (Fig. S-3 in the ESM). Analysis of the TEM images of CdS QDs revealed that the medium diameter of the produced NPs was 2.03 ± 0.32 nm in the absence of H_2O_2. When the concentration of H_2O_2 was 0.03 nm the observed CdS QDs exhibited the medium diameter of 1.29 ± 0.26 nm. In the presence of saturating concentration of H_2O_2 equal to 0.3 mM the absence of CdS QDs were confirmed by TEM.

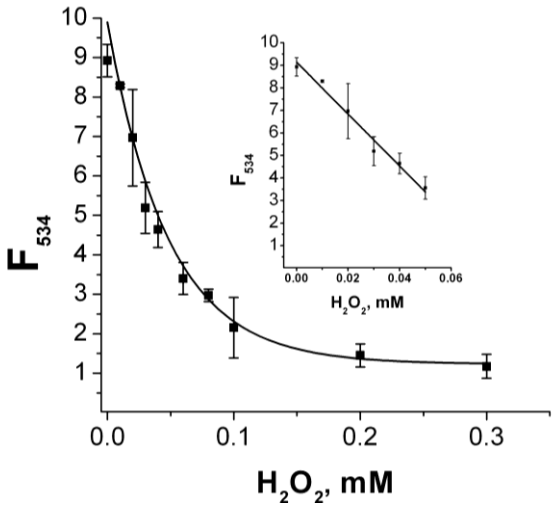

Figure 2. Calibration curve of H_2O_2 obtained using the intensity if the emission peak at 534 nm (F_{534}) The system containing of CSH (0.075 mM), Na_2S (0.1 mM) and $Cd(NO_3)_2$ (1.25 mM), and different concentrations of H_2O_2: a) 0 mM; b) 0.01 mM; c) 0.02 mM; d) 0.03 mM; e) 0.04 mM; f) 0.06 mM; g) 0.08 mM; h) 0.1 mM; i) 0.2 mM; j) 0.3 mM. Inset: linear part of the calibration plot.

3.2. Glucose oxidase assay

The above mentioned fluorogenic method for H_2O_2 detection can be readily combined with enzymatic reactions resulting in the formation of H_2O_2, for example oxidation of enzymatic substrates by oxidases. The operation principle of the fluorogenic assay for evaluation of enzymatic activity of GOx is represented in Scheme 2.

Oxidation of glucose with oxygen catalyzed by GOx ends up in the final products D-glucono 1,5-lactone and H_2O_2. Enzymatically produced H_2O_2 is able to oxidize CSH preventing stabilization and rapid formation of CdS QDs. Fig. 3 shows the emission spectra of CdS QDs formed in the presence of the fixed 1 mM glucose concentration and different concentrations of GOx. As one can see in Figure 3B, the increase in the amount of GOx leads to the decrease in the fluorescence signal as expected for this biocatalytic reaction. We calculated that the LOD of the system was 0.1 μg of GOx per mL. This assay showed 5 times better

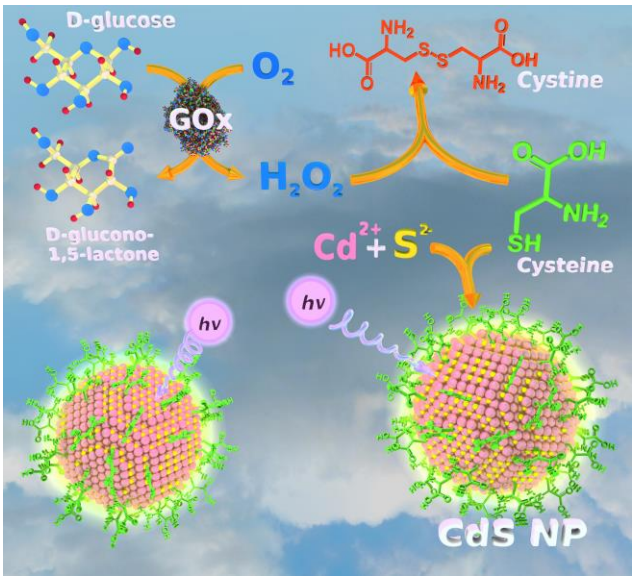

Scheme 2. Fluorometric assay for glucose oxidase activity.

sensitivity that that of the previous published CdS-based fluorogenic assay for GOx [39]. Moreover, this fluorogenic GOx assay is much more sensitive than the colorimetric test for GOx based on CdS NPs [40].

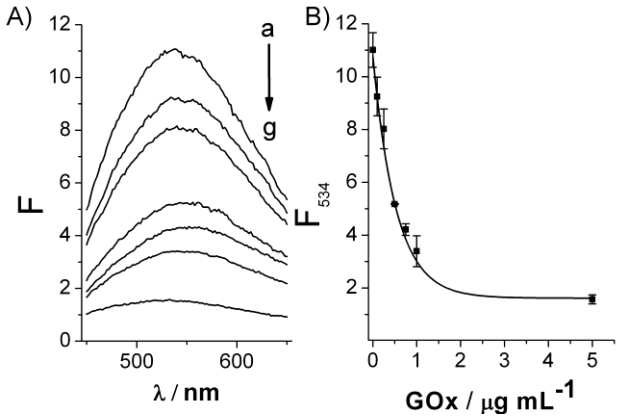

Figure 3. (A) Fluorescence emission spectra of the system containing glucose (1 mM), CSH (0.075 mM), Na_2S (0.1 mM) and $Cd(NO_3)_2$ (1.25 mM) and different concentrations of GOx: a) 0 μg mL^{-1}; b) 0.1 μg mL^{-1}; c) 0.25 μg mL^{-1}; d) 0.5 μg mL^{-1}; e) 0.75 μg mL^{-1}; f) 1 μg mL^{-1}; g) 5 μg mL^{-1}; (B) Calibration curve of GOx obtained using, F_{534}.

We also studied the influence of varying glucose concentrations on the response of our flourogenic assay. Figure 4 shows emission spectra of assay mixtures containing increasing concentrations of glucose and fixed amounts of GOx, CSH, $Cd(NO_3)_2$ and Na_2S. On the basis of the calibration curve in Figure 4.B the LOD of glucose was calculated to be 0.1 mM by UPAC definition [38]. According to the calibration curve (Fig. 4.B) the response to the increasing amounts of glucose was linear within the range from 0 mM to 0.3 mM. Given the fact that the normal level of glucose in human serum published by World Health Organization is < 6.1 mM [41] our assay is even applicable to quantification of glucose in medical laboratories. Therefore, we applied our assay to detection of glucose in human serum employing the standard addition method. In this method several serum sample of the same volume were distributed between different 0.5 mL tubes. The standard known varying amounts of glucose were injected into the samples with human serum. The fluorescence of the samples was measured. The experimental data were plotted with the concentration standards showed in the x-axis and the obtained fluorescence signals in the y-axis of the plot.

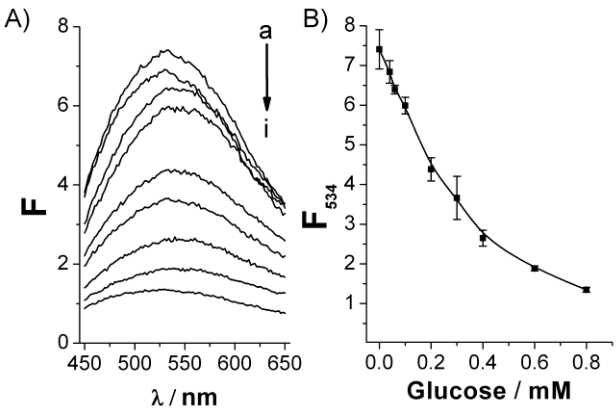

Figure 4. (A) Fluorescence emission spectra of the system containing GOx (5 μg mL^{-1}), CSH (0.075 mM), Na_2S (0.1 mM) and $Cd(NO_3)_2$ (1.25 mM) and different concentrations of glucose: a) 0 mM; b) 0.04 mM; c) 0.06 mM; d) 0.1 mM; e) 0.2 mM; f) 0.3 mM; g) 0.4 mM; h) 0.6 mM; i) 0.8 mM; (B) Calibration curve of glucose obtained using, F_{534}.

The linear regression analysis was performed to calculate the position of the intercept of the calibration line with x-axis, which showed the concentration of glucose in human serum samples (Fig. 5). Taking into consideration all dilutions of the samples, the found concentration of glucose was 6.01 mM. It lies within the limits of normal level of glucose in human serum [41].

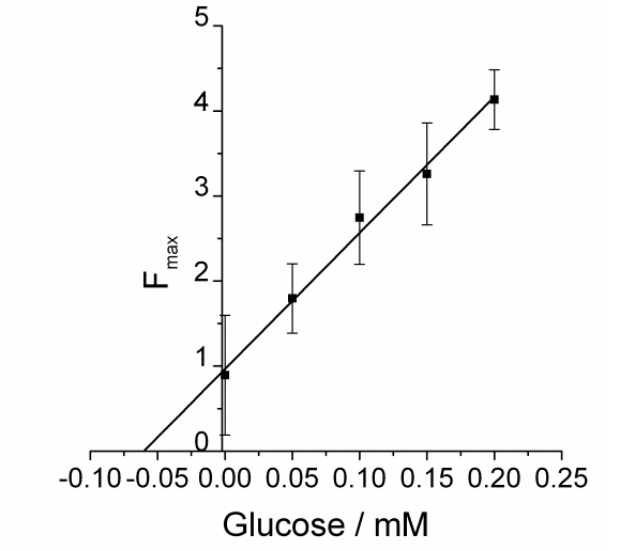

Figure 5. Quantification of glucose in human serum with the method of standard addition. The system contained GOx (5 μg mL^{-1}), CSH (0.075 mM), Na_2S (0.1 mM) and $Cd(NO_3)_2$ (1.25 mM) and various known amounts of added glucose standards.

3.3. Photoelectrochemical detection of glucose

The developed QDs-based PEC system is depicted in Scheme 3. GOx catalyzes oxidation of glucose with oxygen to D-glucono-1,5-lactone and H_2O_2. The former decreases the concentration of CSH modulating the growth of CdS QDs in situ. When the assay solution containing produced CdS QDs is placed over the surface of a SPCE and irradiated with UV light, photons are absorbed by CdS QDs and excite electrons from the occupied valence band (VB) to the empty conduction band (CB) forming electron-hole pairs. CB electrons are transferred from surface of CdS QDs to the electroconductive polymer immobilized on the surface of the SPCE when the positive potential is applied to generate anodic photocurrent. This polymeric electrocatalyst is composed of poly(vinylpyridine) complexed with $Os(bipyridine)_2Cl_2$ (Os–PVP polymer depicted in Fig. S-4 ESM). Holes from VB of CdS QDs are neutralized by the electron donor 1-thioglycerol (TG) which is oxidized to bis(1-thio-2,3 propanediol) at the surface of QDs.

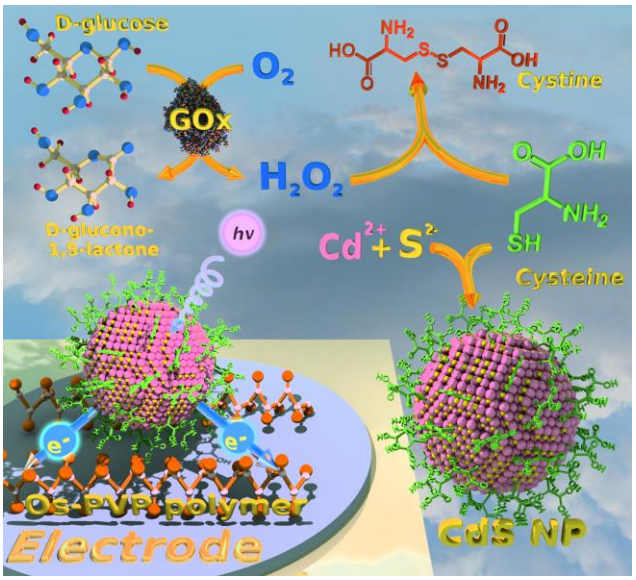

Scheme 3. Electrochemical detection of CdS QDs "wired" by Os-PVP complex to the surface of a SPCE.

In order to photosensitize the surface of SPCE, Os-PVP complex was deposited by cyclic voltammetry (CV) during two cycles in the range from 0 to 0.6 V. After the electrochemical deposition of Os-PVP complex the electrode was washed with water and CV was performed to evaluate the surface coverage of osmium moieties (**Table S-1**). Two redox waves were revealed, confirming that the redox process involves only the central osmium atom (Fig. S-5 ESM). Furthermore, the possible interference from Os-PVP complex with the photocurrent background was assessed at different potentials. The effect of applied potential on the anodic photocurrent is shown in Fig. S-6 (A) ESM. The working potential of 0.3 V *vs.* Ag/AgCl was selected to avoid nonspecific oxidation of TG at the electrode surface. It should be taken into account

that the best ratio of photocurrents registered in the presence and in the absence of CdS QDs (I_{QDs}/I_{Os}) was also achieved at 0.3V *vs.* Ag/AgCl (data not shown)with the signal-to-noise ratio of 3 (S/N = 3). According to the plot representing the effect of different excitation wavelengths on the fluorescence signal (Fig. S-7 ESM), the intensity of the emission peak registered using the excitation wavelength of 365 nm is still higher than 80 % of the maximum emission peak registered using the excitation wavelength of 300 nm. The standard UV illuminator with the maximum output at 365 nm is the most available and inexpensive source of the intense light with the emission peak close to 300 nm therefore it was employed for the photoelectrochemical measurements. All photocurrent responses are presented with the background subtracted at this potential. To estimate the importance of photosensitizing the electrode surface with Os-PVP polymer the control experiment was performed in which non modified SPCE was used for the detection of anodic photocurrent in the presence of CdS QDs and TG in the assay mixture. No significant photocurrent was observed in the absence of Os-PVP polymer on the electrode surface (Fig. S-8 ESM). Thus, Os-PVP polymer is the crucial electrocatalyst mediating the electron transfer of CB electrons from CdS QDs to the SPCE. The photocatalytic oxidation of TG at saturating concentration of 20 mM (Fig. S-9 ESM), which still does not favor its nonspecific electrochemical oxidation, provides the electrons transferred to the surface of the photosensitized SPCEs during quantification of CdS QDs. In the absence of CdS QDs, no significant photocurrent was observed (Figure S-6(B) curve 2).

The influence of the different amounts of glucose on photocurrent is shown in Fig. 6. The decrease in photocurrent is directly related to the increase in the concentration of glucose added to the system. The response shows linearity from 0 to 0.2 mM and saturation starting from 0.4 mM glucose concentration. The LOD was found to be 20 μM (3σ). The average relative standard deviation (RSD) calculated from the glucose calibration plot (obtained using at least three independent SPCEs modified by Os-PVP) was 8%. We also evaluated the response of the system varying the concentration of GOx in the reaction mixture in the presence of 1 mM glucose (Fig. S-10 ESM). According to the calibration curve the LOD was equal to 0.05 μg mL^{-1} (RSD = 4.6%). The control experiments performed in the presence and absence of GOx and glucose showed no significant variation of photocurrent (data no shown).

Comparing with the performance of the fluorogenic method, the PEC system is 5 times more sensitive. Furthermore, the obtained result is also much better than previously published works based on electrochemical detection of glucose, which show worse LODs [42-44].

The standard chromogenic assay for detection of GOx is based on the method previously described in the literature [45]. The chemical interactions employed in the standard commercially available assays:

$$\beta\text{-D-Glucose} + O_2 + H_2O \xrightarrow{GO_x} \text{D-Glucono-1,5-Lactone} + H_2O_2$$

$$H_2O_2 + \text{o-Dianisidine (reduced)} \xrightarrow{HRP} \text{o-Dianisidine (oxidized)}$$

As one can see, this method requires the additional enzyme horseradish peroxidase and very cancerogenic chromogenic dye o-Dianisidine to detect hydrogen peroxide produced by GOx. The commercially available fluorometric kits for detection of GOx (Sigma Aldrich, AbCam) employ fluorogenic substrate of peroxidase 10-acetil-3,7-dihidroxifenoxacina, (AmplexRed®, AbRed®) instead of o-Dianisidine to follow the formation of hydrogen peroxide and require expensive fluorimeters. The dependence of GOx assay on the second enzyme makes the assay prone to errors due to inevitable deactivation of peroxidase even if the components of kits are stored at low temperature.

The photoelectrochemical assay for detection of GOx activity developed by us does require neither expensive fluorogenic dyes nor fluorimeters nor the second enzyme.

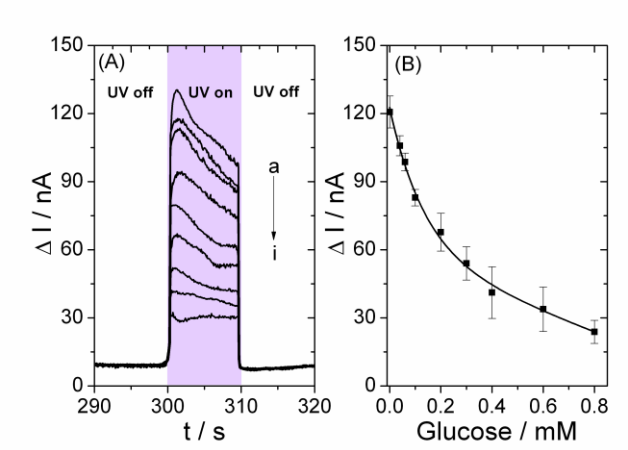

Figure 6. (A) Photocurrent responses of CdS QDs in the system containing GOx (5 μg mL^{-1}), CSH (0.075 mM), TG (20 mM), Na_2S (0.1 mM) and $Cd(NO_3)_2$ (1.25 mM) and different concentrations of glucose: a) 0 mM; b) 0.04 mM; c) 0.06 mM; d) 0.1 mM; e) 0.2 mM; f) 0.3 mM; g) 0.4 mM; h) 0.6 mM; i) 0.8 mM; (B) Calibration curve of GOx obtained at 0.3 V (vs. Ag/AgCl) and 365 nm excitation light.

Finally, the developed sensor was evaluated by the determination of glucose in human serum samples employing the standard addition method. The real samples were not pretreated. As shown in Figure S-6(B) curve 3, electrodes photosensitized with Os-PVP polymer demonstrate a negligible background photocurrent in the presence of human serum samples (around 10 nA) at 0.3V vs. Ag/AgCl. This background current was subtracted from the data of the plot. The known varying amounts of glucose were injected into the samples with human serum. Photocurrents of all samples were measured. The experimental data were plotted with the concentration standards showed in the x-axis and the observed photocurrents in the y-axis of the plot. The intercept of the calibration line with x-axis showing the concentration of glucose in human serum samples was calculated by linear regression (Fig. 7). The found concentration of glucose was 5.06 mM. As reported previously [41], the normal concentration of glucose in human blood is around 5-7 mM. Thus, our device displayed an excellent linear range and RSD values within 10%, showing good sensitivity for detecting glucose.

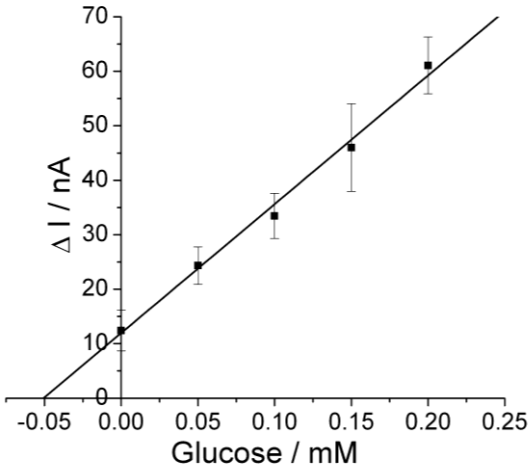

Figure 7. PEC quantification of glucose in human serum with the method of standard addition. The system contained GOx (5 μg mL^{-1}), CSH (0.075 mM), TG (20 mM), Na_2S (0.1 mM) and $Cd(NO_3)_2$ (1.25 mM).

4. Conclusions

The employment of cysteine (CSH) as a capping agent allows for rapid formation of fluorescent CdS QDs in aqueous solutions at room temperature. Hydrogen peroxide (H_2O_2), produced in the course of enzymatic oxidation of D-glucose by glucose oxidase (GOx), oxidizes CSH to cystine (CSSC) modulating the growth of QDs. This biocatalytic process can be applied to the development of simple sensitive fluorometric and photoelectrochemical (PEC) assays for GOx activity in buffered solutions and D-glucose in real samples of human serum using the photocatalytic activity of the resulting QDs. The biocatalytic processes ending up in formation of H_2O_2 are quite abundant in nature. Therefore, we believe that our two model systems potentially can find broad application to

quantify enzymatic activities of many other enzymes generating or consuming H_2O_2.

Acknowledgements

This work was supported by the Spanish Ministry of Economy and Competitiveness (Projects BIO2014-59741-R).

Electronic Supplementary Material: Supplementary material (TEM image of CdS NPs; optimization of CSH concentration; effect of peroxide to preprepared CdS NPs; structure of osmium polymer; control experiments for photoelectrochemical measurements; optimization of 1-thioglycerol concentration; calibration of GOx.) is available in the online version of this article at http://dx.doi.org/10.1007/s12274-***-****-* .

References

[1] Katz, E.; Willner, I. Integrated Nanoparticle–Biomolecule Hybrid Systems: Synthesis, Properties, and Applications. *Angew. Chem., Int. Ed.* **2004**, *43*, 6042-6108.

[2] Liz-Marzán, L. M. Nanometals: Formation and color. *Mater. Today* **2004**, *7*, 26-31.

[3] Li, H.; Xu, D. Silver nanoparticles as labels for applications in bioassays. *TrAC-Trends Anal. Chem.* **2014**, *61*, 67-73.

[4] Omidfar, K.;Khorsand, F.; Darziani Azizi, M. New analytical applications of gold nanoparticles as label in antibody based sensors. *Biosens. Bioelectron.* **2013**, *43*, 336-347.

[5] Mehrabi, M.; Wilson, R. Intercalating gold nanoparticles as universal labels for DNA detection. *Small* **2007**, *3*, 1491-1495.

[6] David, C.;Guillot, N.;Shen, H.;Toury, T.; de la Chapelle, M. L. SERS detection of biomolecules using lithographed nanoparticles towards a reproducible SERS biosensor. *Nanotechnoogyl.* **2010**, *21*, 475501-475507.

[7] Jia, K.;Adam, P. M.;Marks, R. S.; Ionescu, R. E. Fixed Escherichia coli bacterial templates enable the production of sensitive SERS-based gold nanostructures. *Sens. Actuat. B-Chem.* **2015**, *211*, 213-219.

[8] Marks, R. S.; Abdulhalim, I. *Nanomaterials for Water Management: Signal Amplification for Biosensing from Nanostructures*; Pan Stanford: Boca Ratón, 2016.

[9] Jia, K.;Bijeon, J.-L.;Adam, P.-M.; Ionescu, R. E. Large Scale Fabrication of Gold Nano-Structured Substrates Via High Temperature Annealing and Their Direct Use for the LSPR Detection of Atrazine. *Plasmonics* **2013**, *8*, 143–151.

[10] Mayilo, S.;Kloster, M. A.;Wunderlich, M.;Lutich, A.;Klar, T. A.;Nichtl, A.;KÃ¼rzinger, K.;Stefani, F. D.; Feldmann, J. Long-Range Fluorescence Quenching by Gold Nanoparticles in a Sandwich Immunoassay for Cardiac Troponin T. *Nano Lett.* **2009**, *9*, 4558-4563.

[11] Saidi, A.;Mirzaei, M.; Zeinali, S. Using antibody coated gold nanoparticles as fluorescence quenchers for simultaneous determination of aflatoxins (B1, B2) by soft modeling method. *Chemom. Intell. Lab. Syst.* **2013**, *127*, 29-34.

[12] Mirkin, C. A.;Letsinger, R. L.;Mucic, R. C.; Storhoff, J. J. A DNA-based method for rationally assembling nanoparticles into macroscopic materials. *Nature* **1996**, *382*, 607-609.

[13] Pavlov, V.;Xiao, Y.;Shlyahovsky, B.; Willner, I. Aptamer-functionalized Au nanoparticles for the amplified optical detection of thrombin. *J. Am. Chem. Soc.* **2004**, *126*, 11768-11769.

[14] Xiao, Y.;Pavlov, V.;Shlyahovsky, B.; Willner, I. An Os(II)--bisbipyridine--4-picolinic acid complex mediates the biocatalytic growth of au nanoparticles: optical detection of glucose and acetylcholine esterase inhibition. *Chem.-Eur. J.* **2005**, *11*, 2698-2704.

[15] Fanjul-Bolado, P.;Hernandez-Santos, D.;Gonzalez-Garcia, M. B.; Costa-Garcia, A. Alkaline phosphatase-catalyzed silver deposition for electrochemical detection. *Anal. Chem.* **2007**, *79*, 5272-5277.

[16] Shlyahovsky, B.;Katz, E.;Xiao, Y.;Pavlov, V.; Willner, I. Optical and Electrochemical Detection of NADH and of NAD+-Dependent Biocatalyzed Processes by the Catalytic Deposition of Copper on Gold Nanoparticles. *Small* **2005**, *1*, 213-216.

[17] Pavlov, V. Enzymatic Growth of Metal and

Semiconductor Nanoparticles in Bioanalysis. *Part. Part. Syst. Charact.* **2013**, *31*, 36-45.

[18] Merkoçi, A. *Biosensing Using Nanomaterials*; John Wiley & Sons, Inc., 2009.

[19] Garai-Ibabe, G.;Saa, L.; Pavlov, V. Enzymatic product-mediated stabilization of CdS quantum dots produced in situ: application for detection of reduced glutathione, NADPH, and glutathione reductase activity. *Anal. Chem.* **2013**, *85*, 5542-5546.

[20] Saa, L.;Mato, J. M.; Pavlov, V. Assays for methionine gamma-lyase and S-adenosyl-L-homocysteine hydrolase based on enzymatic formation of CdS quantum dots in situ. *Anal. Chem.* **2012**, *84*, 8961-8965.

[21] Chatterjee, A.;Priyam, A.;Das, S. K.; Saha, A. Size tunable synthesis of cysteine-capped CdS nanoparticles by gamma-irradiation. *J. Colloid. Interf. Sci.* **2006**, *294*, 334-342.

[22] Kumar, P.;Kumar, P.;Bharadwaj, L. M.;Paul, A. K.;Sharma, S. C.;Kush, P.; Deep, A. Aqueous Synthesis of l-Cysteine Stabilized Water-Dispersible CdS:Mn Quantum Dots for Biosensing Applications. *BioNanoSci.* **2013**, *3*, 95-101.

[23] Luo, D.;Smith, S. W.; Anderson, B. D. Kinetics and mechanism of the reaction of cysteine and hydrogen peroxide in aqueous solution. *J. Pharm. Sci.* **2005**, *94*, 304-316.

[24] Winterbourn, C. C.; Metodiewa, D. Reactivity of biologically important thiol compounds with superoxide and hydrogen peroxide. *Free Radical Biol. Med.* **1999**, *27*, 322-328.

[25] Barton, J. P.;Packer, J. E.; Sims, R. J. Kinetics of the reaction of hydrogen peroxide with cysteine and cysteamine. *J. Chem. Soc., Perkin Trans. 2* **1973**, 1547-1549.

[26] Bankar, S. B.;Bule, M. V.;Singhal, R. S.; Ananthanarayan, L. Glucose oxidase--an overview. *Biotechnol. Adv.* **2009**, *27*, 489-501.

[27] Zhao, W.-W.;Xu, J.-J.; Chen, H.-Y. Photoelectrochemical bioanalysis: the state of the art. *Chem. Soc. Rev.* **2015**, *44*, 729-741.

[28] Devadoss, A.;Sudhagar, P.;Terashima, C.;Nakata, K.; Fujishima, A. Photoelectrochemical biosensors: New insights into promising photoelectrodes and signal amplification strategies. *J. Photochem. Photobiol., C* **2015**, *24*, 43-63.

[29] Yue, Z.;Lisdat, F.;Parak, W. J.;Hickey, S. G.;Tu, L.;Sabir, N.;Dorfs, D.; Bigall, N. C. Quantum-Dot-Based Photoelectrochemical Sensors for Chemical and Biological Detection. *ACS Appl. Mater. Interfaces* **2013**, *5*, 2800-2814.

[30] Zhou, H.;Liu, J.; Zhang, S. Quantum dot-based photoelectric conversion for biosensing applications. *TrAC-Trends Anal. Chem* **2015**, *67*, 56-73.

[31] Zhao, W.-W.;Wang, J.;Zhu, Y.-C.;Xu, J.-J.; Chen, H.-Y. Quantum Dots: Electrochemiluminescent and Photoelectrochemical Bioanalysis. *Anal. Chem.* **2015**, *87*, 9520-9531.

[32] Walcarius, A. Electrocatalysis, sensors and biosensors in analytical chemistry based on ordered mesoporous and macroporous carbon-modified electrodes. *TrAC-Trends Anal. Chem.* **2012**, *38*, 79-97.

[33] Long, Y.-T.;Kong, C.;Li, D.-W.;Li, Y.;Chowdhury, S.; Tian, H. Ultrasensitive Determination of Cysteine Based on the Photocurrent of Nafion-Functionalized CdS–MV Quantum Dots on an ITO Electrode. *Small* **2011**, *7*, 1624-1628.

[34] Zhao, W.-W.;Ma, Z.-Y.;Yan, D.-Y.;Xu, J.-J.; Chen, H.-Y. In Situ Enzymatic Ascorbic Acid Production as Electron Donor for CdS Quantum Dots Equipped TiO2 Nanotubes: A General and Efficient Approach for New Photoelectrochemical Immunoassay. *Anal. Chem.* **2012**, *84*, 10518-10521.

[35] Zhou, H.; Liu, J.; Zhang, S. Quantum dot-based photoelectric conversion for biosensing applications. *TrAC-Trends Anal. Chem.* **2015**, *67*, 56-73.

[36] Iyer, R.; Pavlov, V.;Katakis, I.; Bachas, L. G. Amperometric Sensing at High Temperature with a "Wired" Thermostable Glucose-6-phosphate Dehydrogenase from Aquifex aeolicus. *Anal. Chem.* **2003**, *75*, 3898-3901.

[37] Vreeke, M. S.;Yong, K. T.; Heller, A. A Thermostable Hydrogen Peroxide Sensor Based on "Wiring" of Soybean Peroxidase. *Anal. Chem.* **1995**, *67*, 4247-4249.

[38] McNaught, A. D.; Wilkinson, A. IUPAC Compendium of

Chemical Terminology. . In *Gold Book*; Oxford, UK, 1997.

[39] Saa, L.; Pavlov, V. Enzymatic growth of quantum dots: applications to probe glucose oxidase and horseradish peroxidase and sense glucose. *Small* **2012**, *8*, 3449-3455.

[40] Grinyte, R.;Garai-Ibabe, G.;Saa, L.; Pavlov, V. Application of photocatalytic cadmium sulfide nanoparticles to detection of enzymatic activities of glucose oxidase and glutathione reductase using oxidation of 3,3',5,5'-tetramethylbenzidine. *Anal. Chim. Acta* **2015**, *881*, 131-138.

[41] Rodriguez, B. L.;Abbott, R. D.;Fujimoto, W.;Waitzfelder, B.;Chen, R.;Masaki, K.;Schatz, I.;Petrovitch, H.;Ross, W.;Yano, K.;Blanchette, P. L.; Curb, J. D. The American Diabetes Association and World Health Organization Classifications for Diabetes. In *Their impact on diabetes prevalence and total and cardiovascular disease mortality in elderly Japanese-American men*, 2002; pp 951-955.

[42] Li, W.;Qian, D.;Wang, Q.;Li, Y.;Bao, N.;Gu, H.; Yu, C. Fully-drawn origami paper analytical device for electrochemical detection of glucose. *Sens. Actuat. B-Chem.* **2016**, *231*, 230-238.

[43] Li, L.;Liang, B.;Li, F.;Shi, J.;Mascini, M.;Lang, Q.; Liu, A. Co-immobilization of glucose oxidase and xylose dehydrogenase displayed whole cell on multiwalled carbon nanotube nanocomposite films modified electrode for simultaneous voltammetric detection of d-glucose and d-xylose. *Biosens. Bioelectron.* **2013**, *42*, 156-162.

[44] Tanne, J.;Schäfer, D.;Khalid, W.;Parak, W. J.; Lisdat, F. Light-Controlled Bioelectrochemical Sensor Based on CdSe/ZnS Quantum Dots. *Anal. Chem.* **2011**, *83*, 7778-7785.

[45] Bergmeyer, H. U., Gawehn, K., Grassl, M. *Methods of Enzymatic Analysis*; Academic Press: New York, 1974.

.

Electronic Supplementary Material

Modulation of Growth of Cysteine-capped Cadmium Sulphide Quantum Dots with Enzymatically produced Hydrogen Peroxide

Ruta Grinyte[1], Javier Barroso[1], Laura Saa[1], Valeri Pavlov[1] ✉

[1] Biosensing Unit, CIC BiomaGUNE, Parque Tecnológico de San Sebastian, Paseo Miramón 182, Donostia-San Sebastián, 20009 Spain

Supporting information to DOI 10.1007/s12274-****-****-* (automatically inserted by the publisher)

List of Electronic Supplementary Material:

Address correspondence to Valeri Pavlov, vpavlov@cicbiomagune.es

1. Optical method

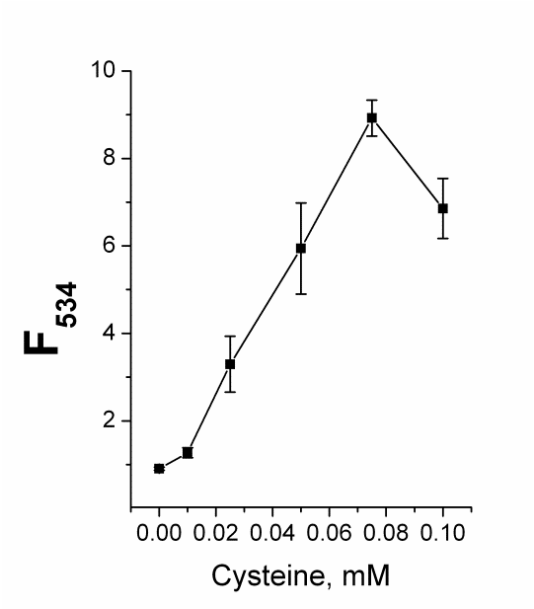

Fig. S-1 Effect of cysteine concentration on fluorescence intensity in the reaction mixture composed of Na_2S 0.1 mM and $Cd(NO_3)_2$ 1.25 mM. Incubation time 5 min, λ_{exc} = 300 nm.

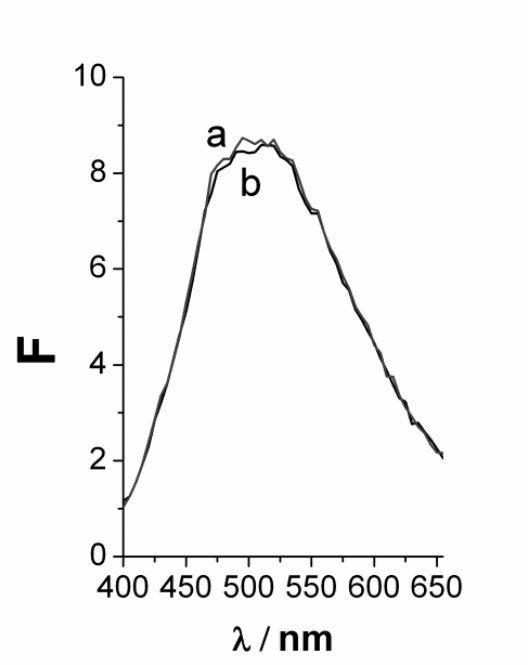

Fig. S-2 The system containing cysteine-stabilized CdS QDs before addition of H_2O_2 (curve a) and after addition of 0.1 mM of H_2O_2 (curve b). Incubation time 5 min, λ_{exc} = 300 nm.

2. TEM images of CdS QDs and size distribution

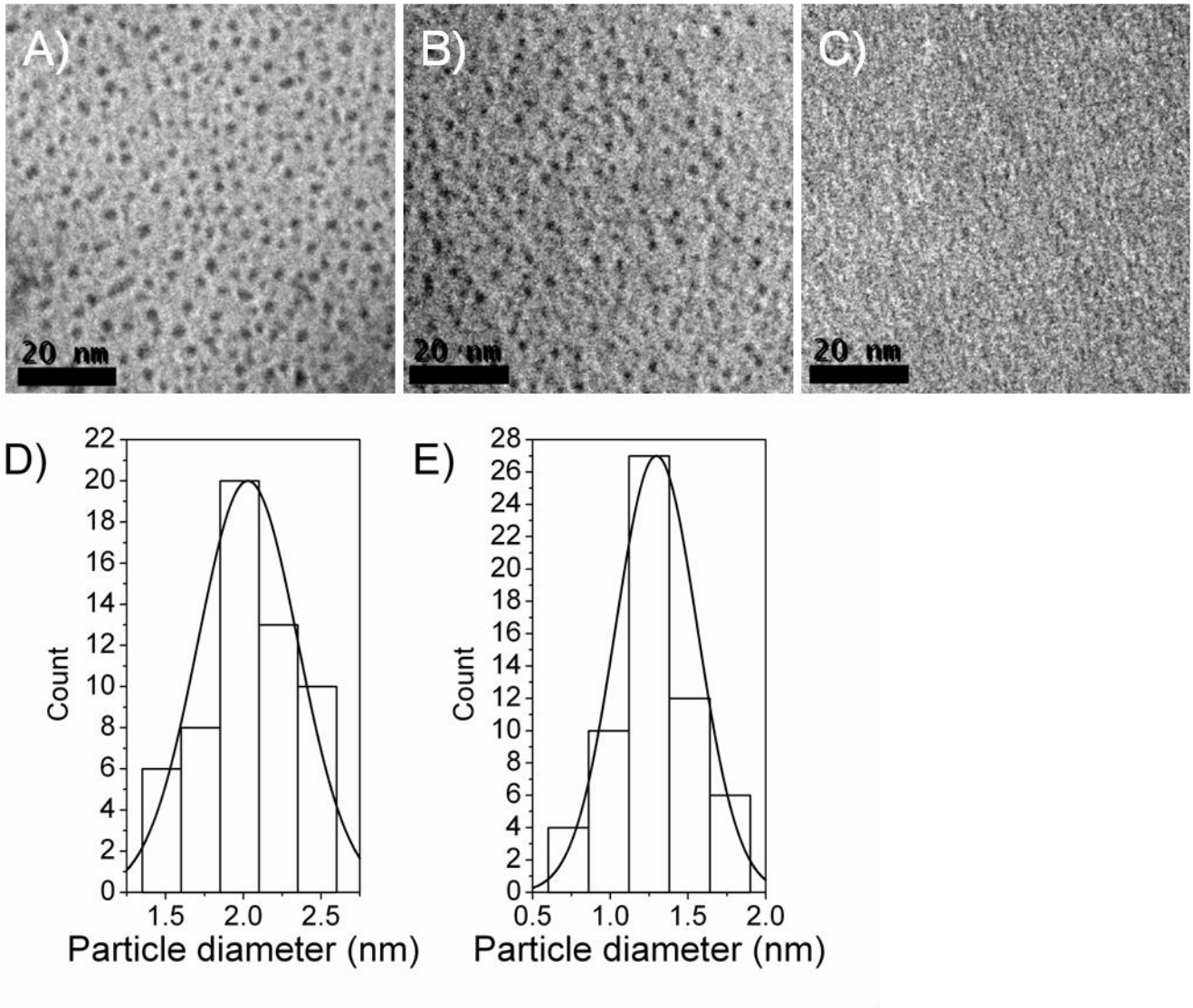

Fig. S-3 TEM images of cysteine stabilized CdS QDs in the presence of (A) 0 mM of H_2O_2 (B) 0.03 mM of H_2O_2 (C) 0.3 mM of H_2O_2; Size distribution of cysteine stabilized CdS QDs in the presence of (D) 0 mM of H_2O_2 (E) 0.03 mM of H_2O_2.

3.- Structure of osmium polymer

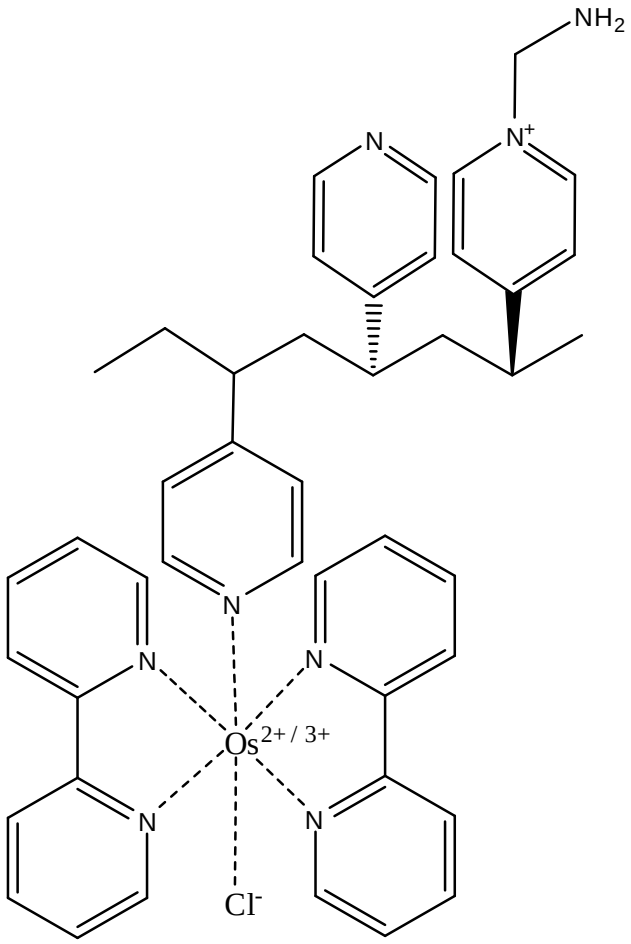

Fig. S-4. 2D structure of poly(vinypyridine) complexed with Os(bipyridine)$_2$Cl$_2$ (Os-PVP complex).

The polymer was synthesized according to the procedure previously published elsewhere (Katakis I., Ye L., Heller A., 1994. J. Am. Chem. Soc. 116, 3617-3618).

4. Electrochemical characterization of SPCEs

Surface coverage (Γ) of electroactive species was determined by cyclic voltammetry (CV) calculating the charge under the areas of peaks depicted in Fig. S5.

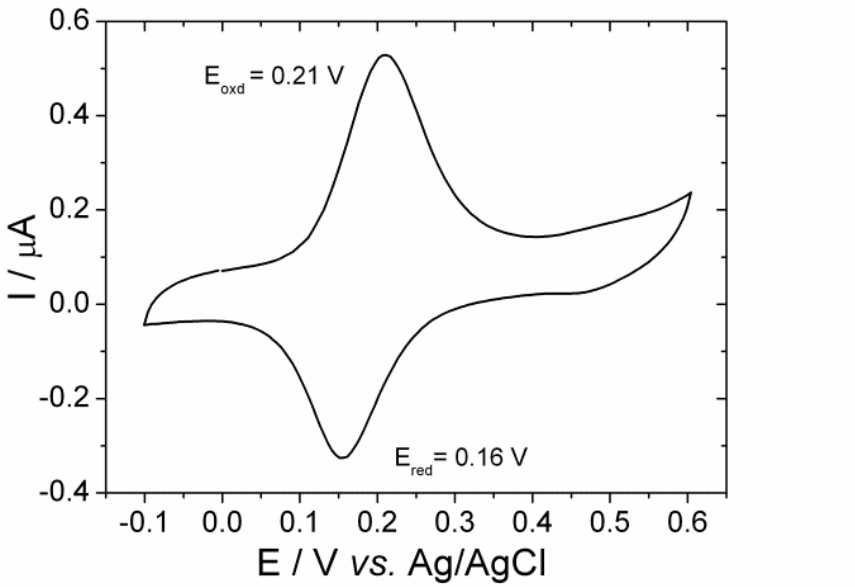

Fig. S-5 Cyclic voltammograms of screen-pirnted carbon electrode (SPCE) modified by Os-PVP complex. Scan rate of 50 mV s^{-1}.

Taking into account the number of exchanged electrons per redox molecule and the Faraday´s constant, the surface concentration was calculated. The peak intensity, I_p, is a function of scan rate υ, charge diffusion coefficient D_0, number of exchanged electrons n, surface concentration of redox active species C_0^*, surface coverage Γ, electrode surface area A, temperature T, Faraday´s constant F and gas constant R according to the equation:

$$I_p = n^2F^2\Gamma A\upsilon(4RT)^{-1}$$

The Randles-Sevčik equation for quasi-reversible electron transfer processes was employed to determine the active electrode area, as follows:

$$I_p = (2.65 * 10^5)n^{3/2}ACD^{1/2}\upsilon^{1/2}$$

where n is the number of electrons participating in the redox process, A is the active electrode area, D is the diffusion coefficient, C is the concentration of probe molecule and υ is the scan rate. The CV were performed in potasium ferricyanide (2mM). The calculations of active area (A) were carried out employing the value of D mentioned by Kadara et al., 2009. The electrochemically active area was 0.099 cm^2. The surface coverage is shown in Table S-1 for three independent screen-printed carbon electrodes (SPCEs) modified by Os-PVP complex. The average coverage was found to be 10.9 ± 1.4 nmol cm^{-2}.

Table S-1 Surface coverage (Γ / nmol cm^{-2}) of three independent screen-printed carbon electrodes.

Electrode	Γ / nmol cm^{-2}
1	**11.2**
2	**12.1**
3	**9.4**

References

1. Prodromidis M.I., Florou A.B., Tzouwara-Karayanni S.M., Karayannis M.I., 2000. Electroanal. 12, 1498-1501.
2. Gao Z., Binyamin G., Kim H.H., Barton S.C., Zhang Y., Heller A., 2002. Angew. Chem. Int. Ed. 41, 810-813.
3. Kadara R.O., Jenkinson N., Banks C.E., 2009. Sensor Actuat B-Chem. 138,556–562.

5. Photoelectrochemical control

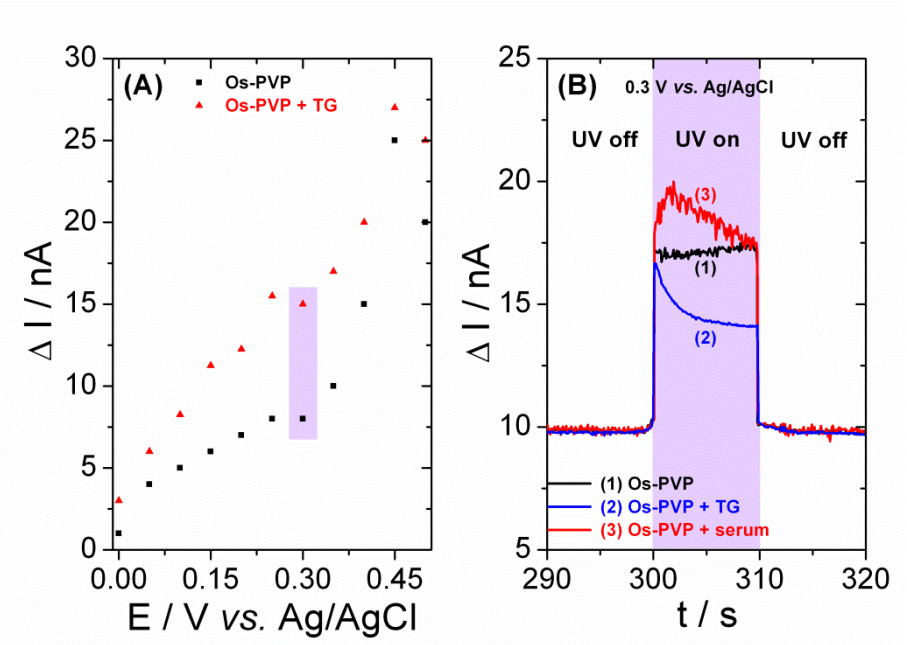

Fig. S-6 (A) Variation in the photocurrent for the modified SPCE sensitized by conductive OS-PVP complex in the presence and in the absence of 1-thioglycerol (TG) in the potential range between from 0 to 0.5 V vs. Ag/AgCl; (B) Photocurrent background responses in the absence of CdS QDs on the SPCE containing (1) only Os-PVP complex; (2) Os-PVP complex, 1-thioglycerol (TG) 20 mM and (3) Os-PVP complex, human serum.

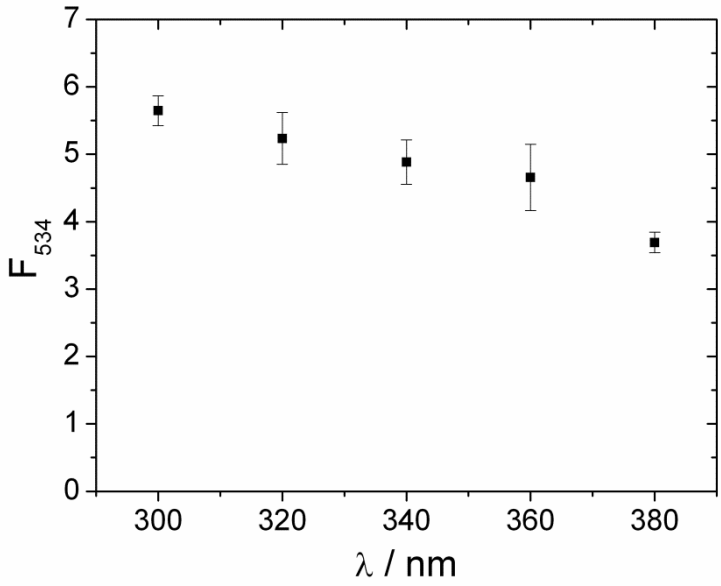

Fig. S-7 The plot showing the dependence of the emission light intensity, registered in the reaction mixture containing CdS QDs, on the wavelength of the excitation light.

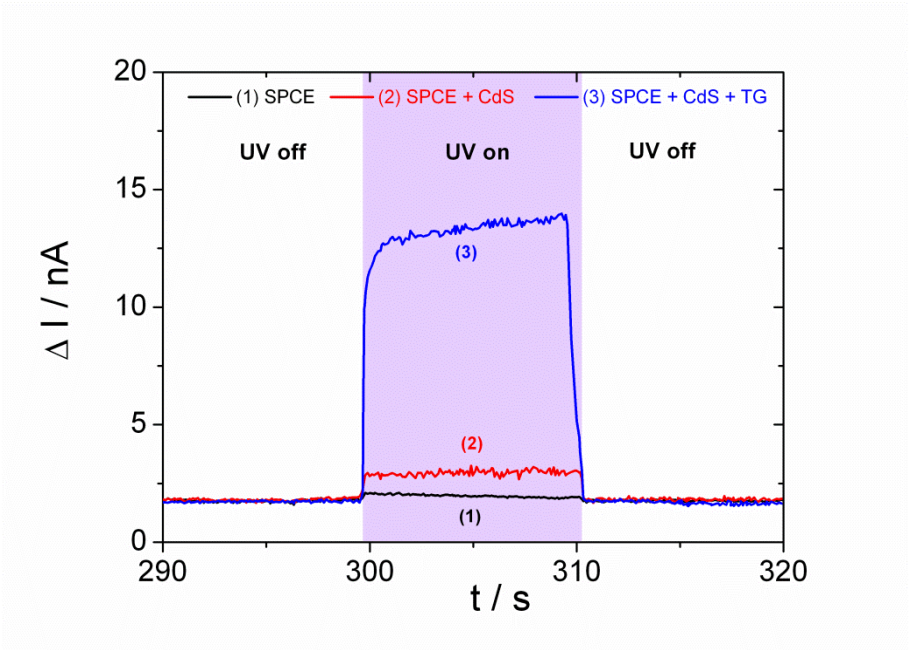

Fig. S-8 Photocurrent background responses in the absence of Os-PVP complex for (1) only SPCE; (2) SPCE and CdS QDs and (3) SPCE, CdS QDs and 1-thioglycerol (TG) 20 mM.

6. Optimization of 1-thioglycerol concentration

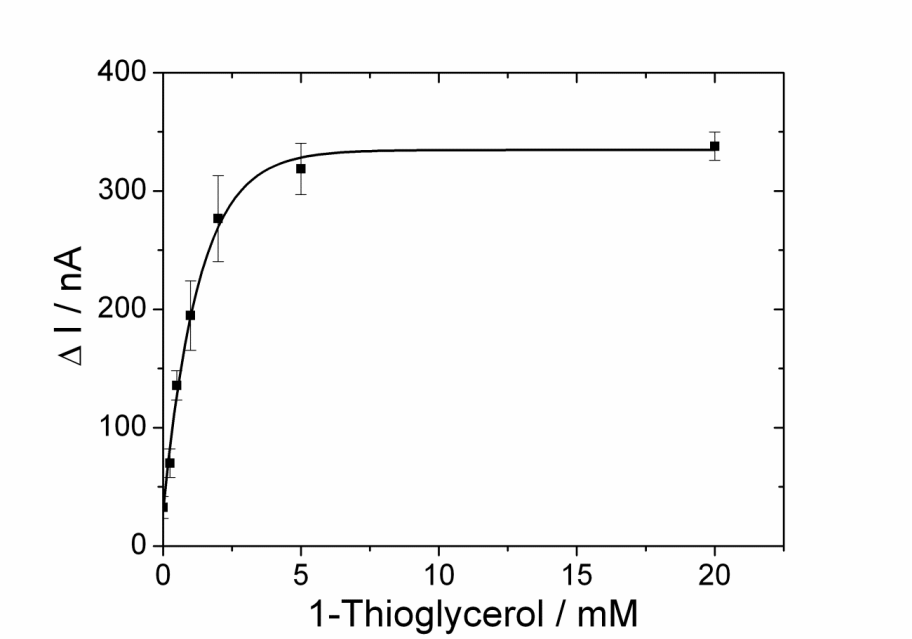

Figure S-9 Effect of the increasing 1-thioglycerol concentrations (TG) on photocurrent observed in the presence of CdS QDs at 0.3 V (*vs.* Ag/AgCl) and 365 nm excitation light. Concentrations of TG: a) 0 mM; b) 0.25 mM; c) 0.5 mM; d) 1 mM; e) 2 mM; f) 5 mM; g) 20 mM. The the system contains $Cd(NO_3)_2$ (1.25 mM), Na_2S (0.1 mM) and cysteine (0.075 mM). The average relative standard deviation (RSD) calculated from the plot (obtained using at least three independent SPCEs modified by Os-PVP) was 9.75 %.

7. Optimization of glucose oxidase concentration for photoelectrochemical measurements

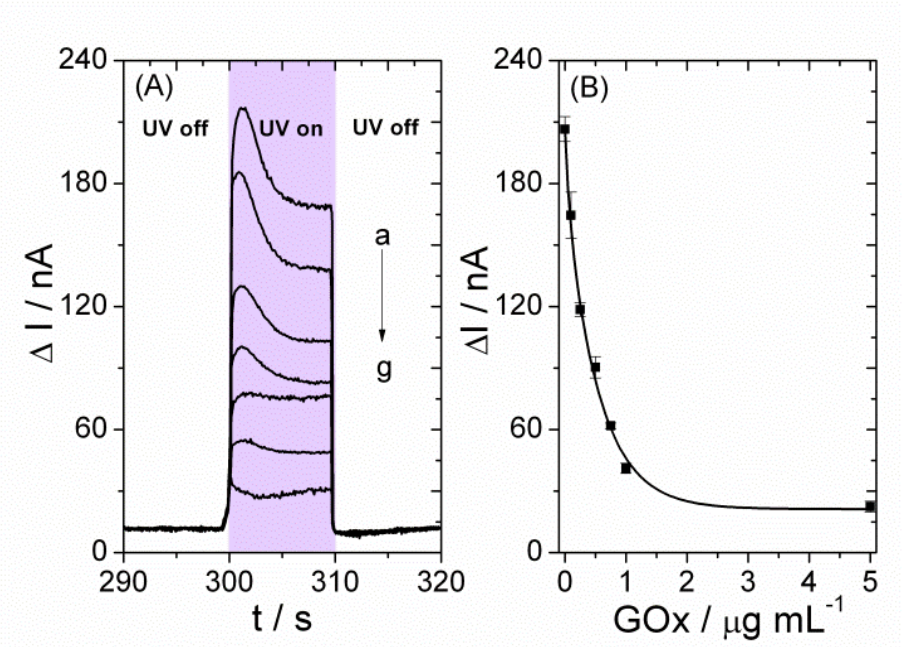

Fig. S-10 (A) Photocurrent responses of the system containing glucose (1 mM), cysteine (0.075 mM), 1-thioglycerol (TG) 20 mM, Na_2S (0.1 mM) and $Cd(NO_3)_2$ (1.25 mM) and different concentrations of GOx: a) 0 μg mL^{-1}; b) 0.1 μg mL^{-1}; c) 0.25 μg mL^{-1}; d) 0.5 μg mL^{-1}; e) 0.75 μg mL^{-1}; f) 1 μg mL^{-1}; g) 5 μg mL^{-1}; (B) Calibration curve of GOx obtained at 0.3 V (vs. Ag/AgCl) and 365 nm excitation light.

Figure

FIGURES AND SCHEMES

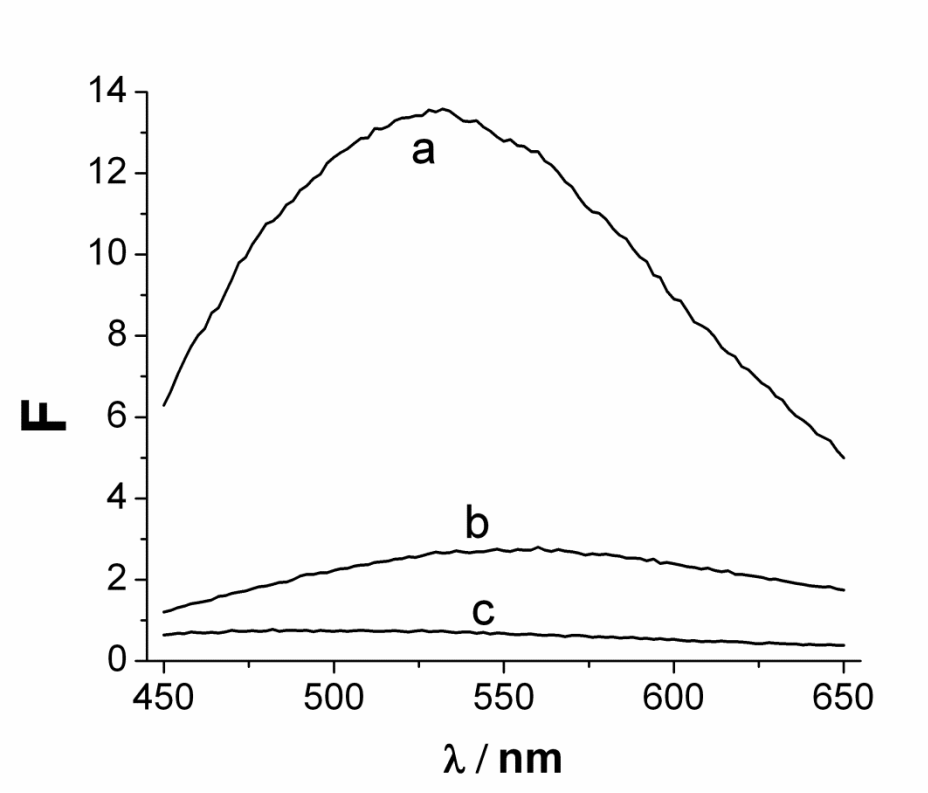

Figure 1. Fluorescence emission spectra of the system containing (a) CSH (0.5 mM), Na_2S (0.1 mM), $Cd(NO_3)_2$ (1.25 mM); (b) CSSC (0.5 mM), Na_2S (0.1 mM), $Cd(NO_3)_2$ (1.25 mM); (c) only Na_2S (0.1 mM) and $Cd(NO_3)_2$ (1.25 mM).

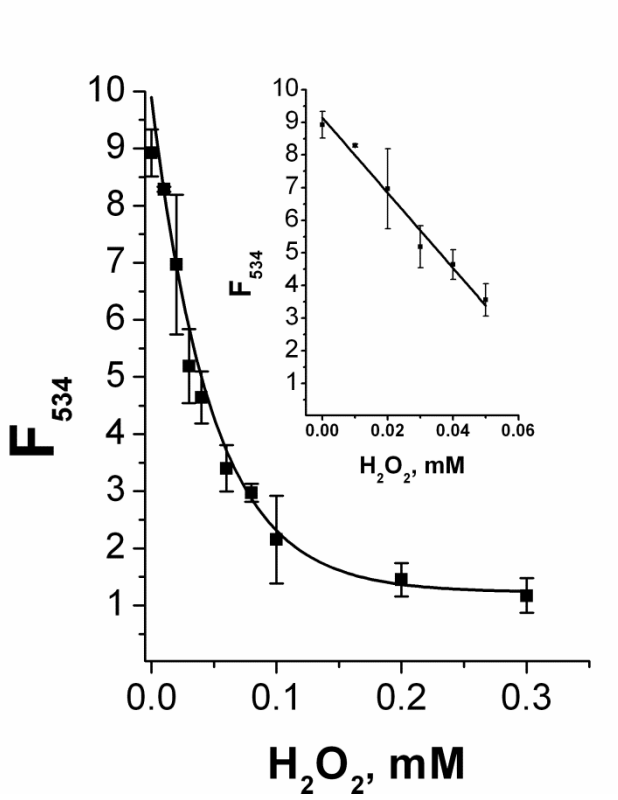

Figure 2. Calibration curve of H_2O_2 obtained using the intensity if the emission peak at 534 nm (F_{534}) The system containing of CSH (0.075 mM), Na_2S (0.1 mM) and $Cd(NO_3)_2$ (1.25 mM), and different concentrations of H_2O_2: a) 0 mM; b) 0.01 mM; c) 0.02 mM; d) 0.03 mM; e) 0.04 mM; f) 0.06 mM; g) 0.08 mM; h) 0.1 mM; i) 0.2 mM; j) 0.3 mM. Inset: linear part of the calibration plot.

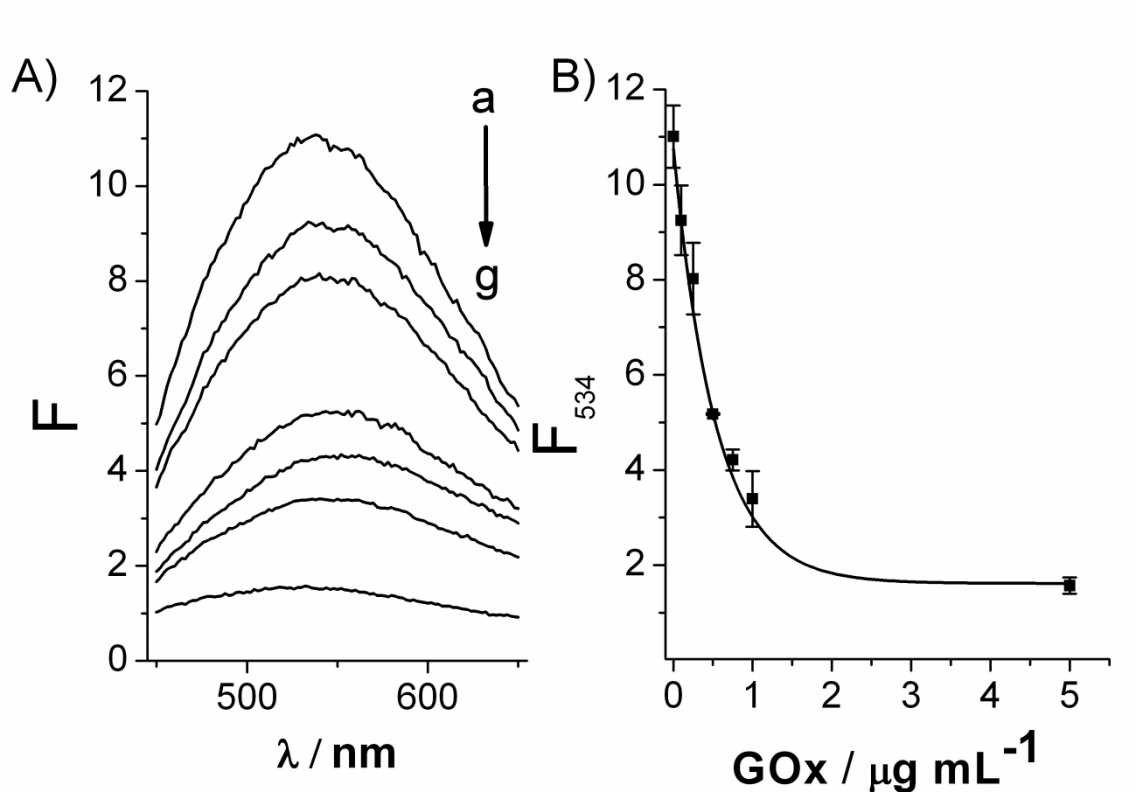

Figure 3. (A) Fluorescence emission spectra of the system containing glucose (1 mM), CSH (0.075 mM), Na_2S (0.1 mM) and $Cd(NO_3)_2$ (1.25 mM) and different concentrations of GOx: a) 0 μg mL^{-1}; b) 0.1 μg mL^{-1}; c) 0.25 μg mL^{-1}; d) 0.5 μg mL^{-1}; e) 0.75 μg mL^{-1}; f) 1 μg mL^{-1}; g) 5 μg mL^{-1}; (B) Calibration curve of GOx obtained using, F_{534}.

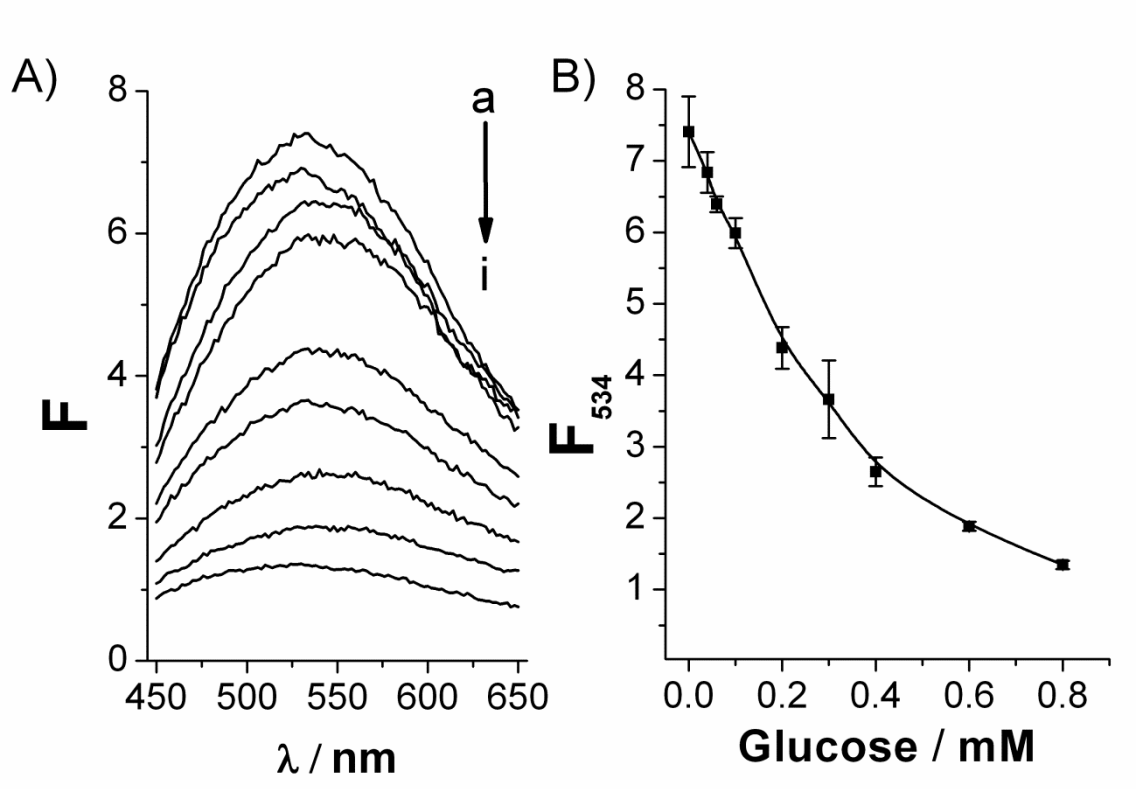

Figure 4. (A) Fluorescence emission spectra of the system containing GOx (5 μg mL^{-1}), CSH (0.075 mM), Na_2S (0.1 mM) and $Cd(NO_3)_2$ (1.25 mM) and different concentrations of glucose: a) 0 mM; b) 0.04 mM; c) 0.06 mM; d) 0.1 mM; e) 0.2 mM; f) 0.3 mM; g) 0.4 mM; h) 0.6 mM; i) 0.8 mM; (B) Calibration curve of glucose obtained using, F_{534}.

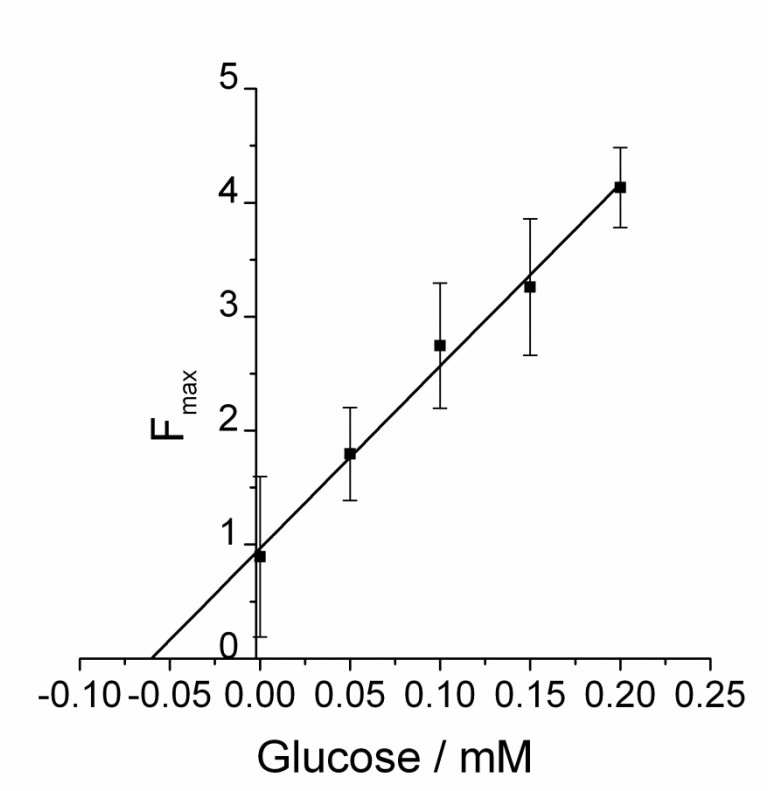

Figure 5. Quantification of glucose in human serum with the method of standard addition. The system contained GOx (5 μg mL^{-1}), CSH (0.075 mM), Na_2S (0.1 mM) and $Cd(NO_3)_2$ (1.25 mM) and various known amounts of added glucose standards.

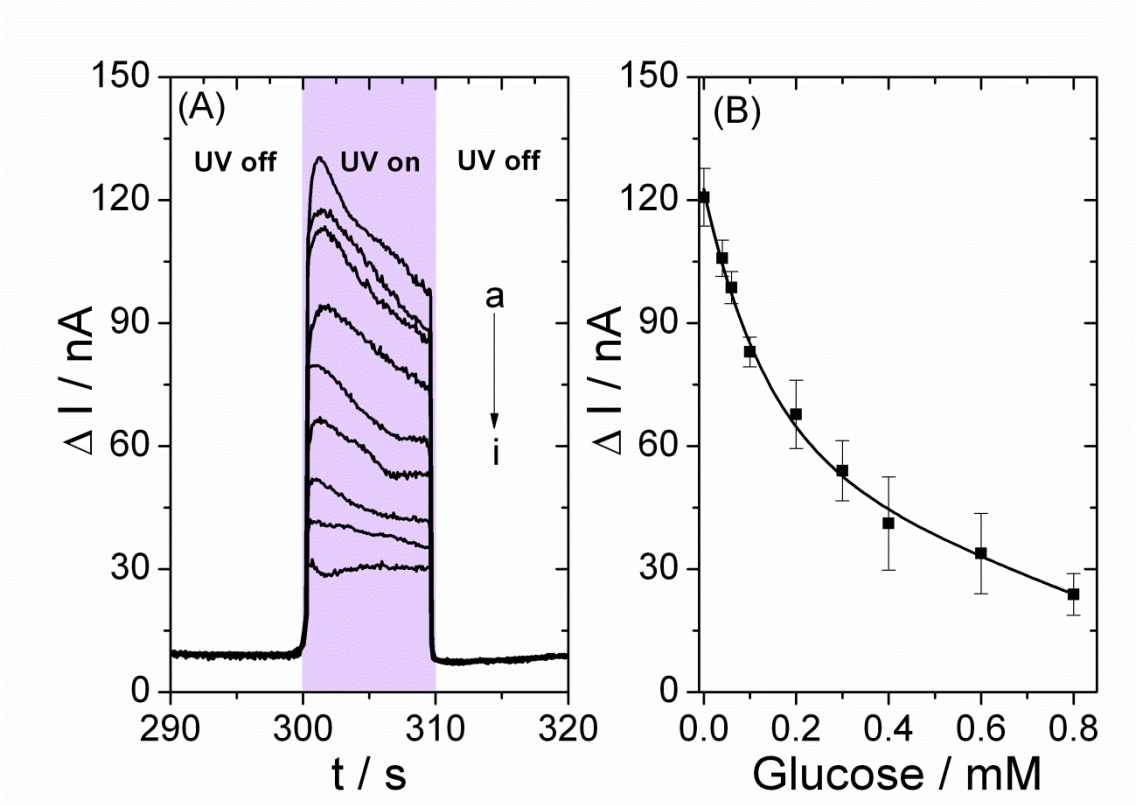

Figure 6. (A) Photocurrent responses of CdS QDs in the system containing GOx (5 μg mL^{-1}), CSH (0.075 mM), TG (20 mM), Na_2S (0.1 mM) and $Cd(NO_3)_2$ (1.25 mM) and different concentrations of glucose: a) 0 mM; b) 0.04 mM; c) 0.06 mM; d) 0.1 mM; e) 0.2 mM; f) 0.3 mM; g) 0.4 mM; h) 0.6 mM; i) 0.8 mM; (B) Calibration curve of GOx obtained at 0.3 V (vs. Ag/AgCl) and 365 nm excitation light.

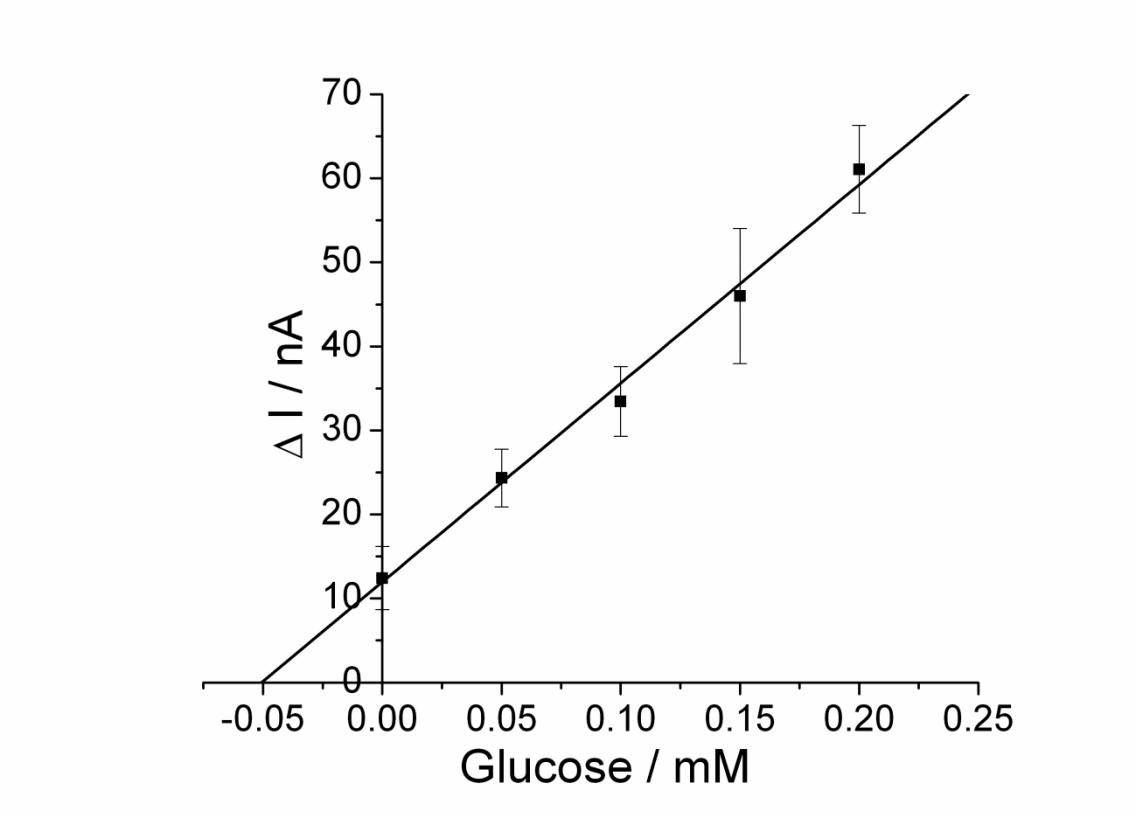

Figure 7. PEC quantification of glucose in human serum with the method of standard addition. The system contained GOx (5 μg mL^{-1}), CSH (0.075 mM), TG (20 mM), Na_2S (0.1 mM) and $Cd(NO_3)_2$ (1.25 mM).

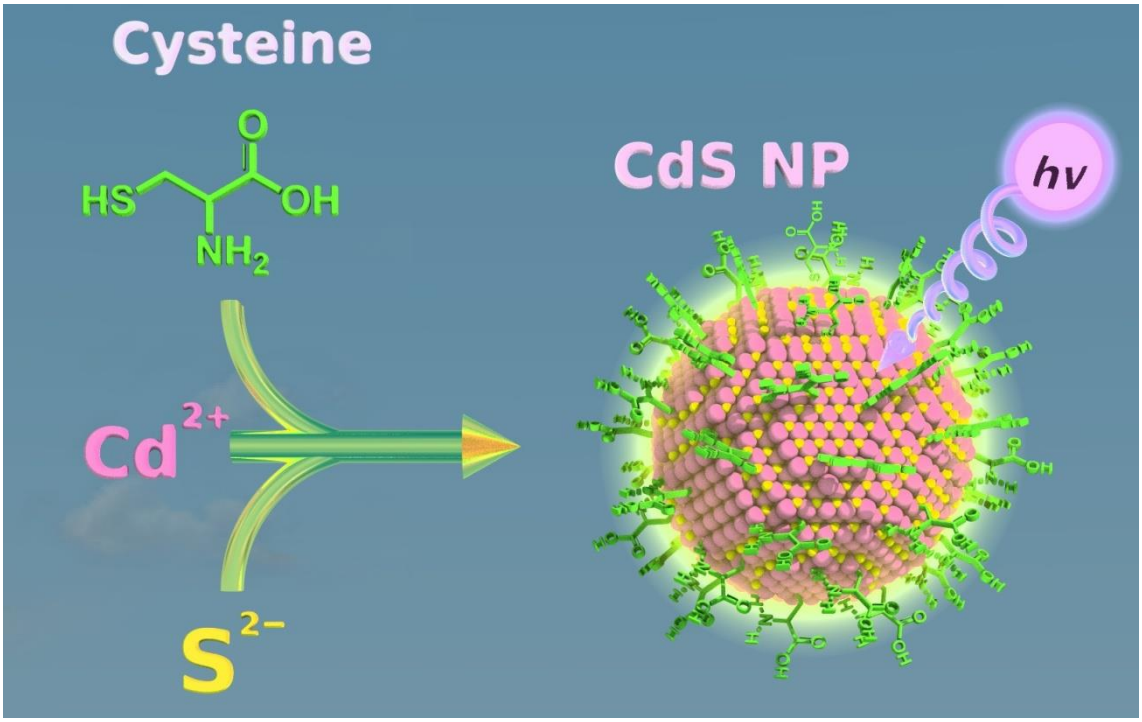

Scheme 1. Modulation of CdS QDs growth with cysteine.

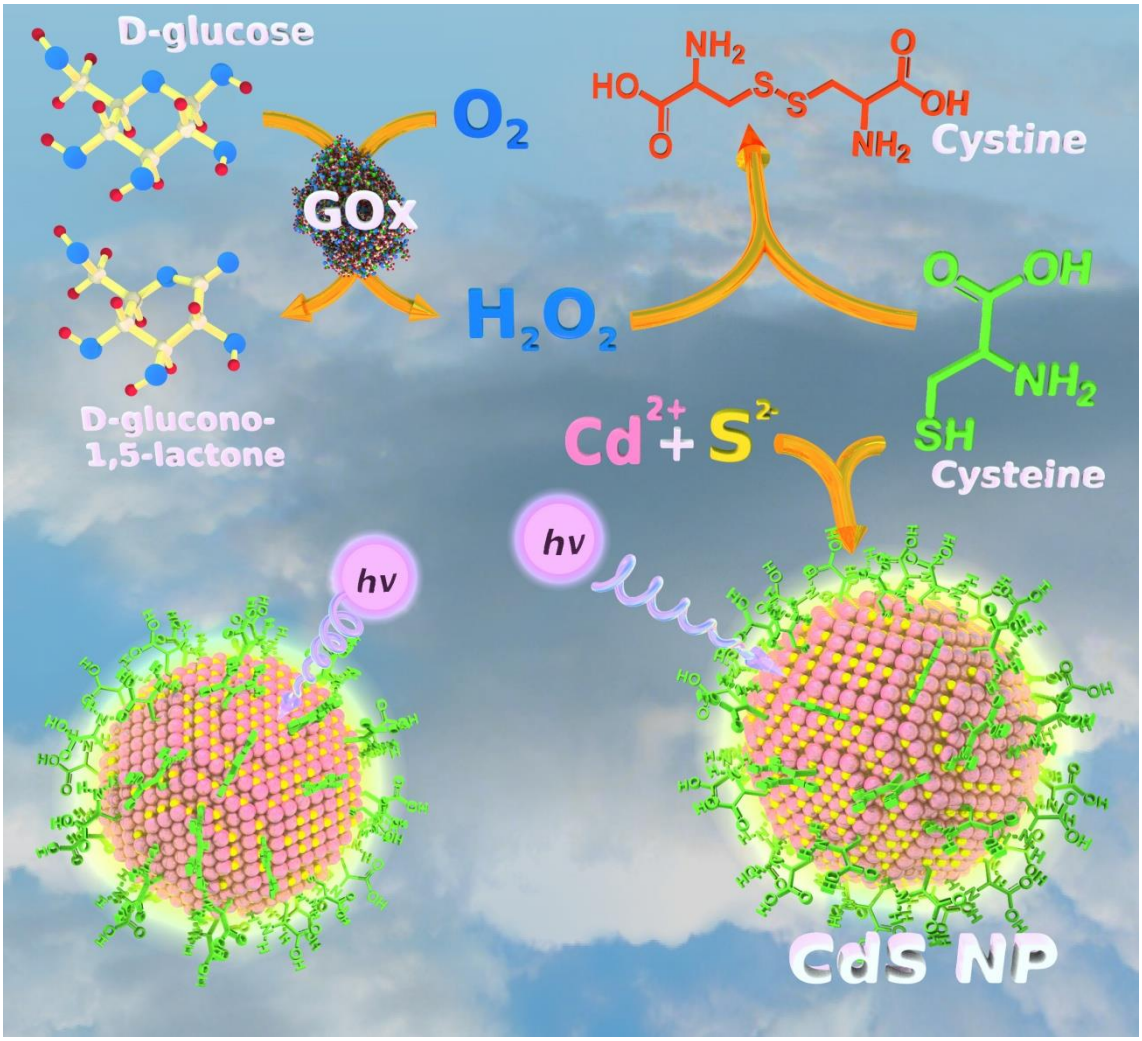

Scheme 2. Fluorometric assay for glucose oxidase activity.

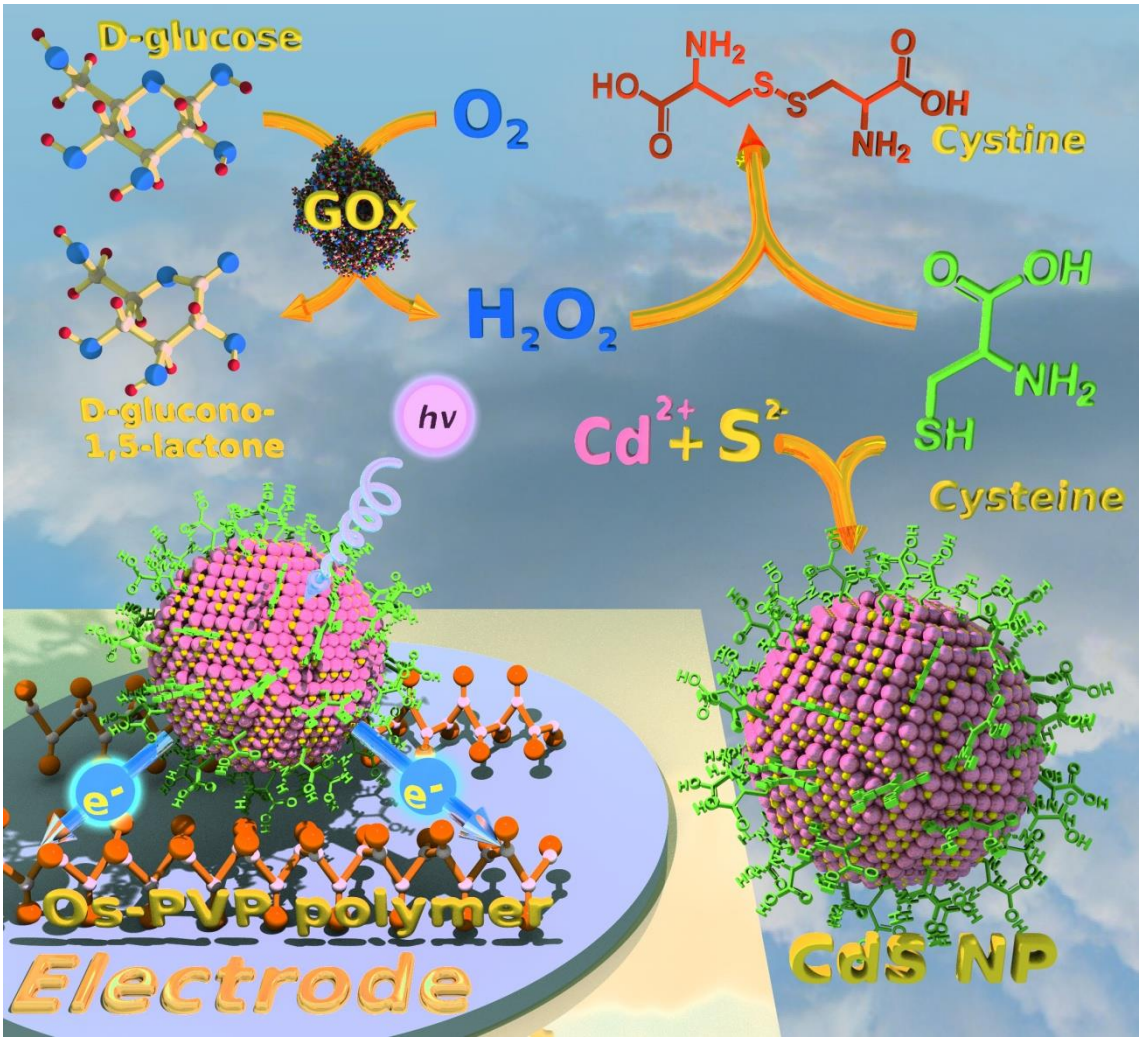

Scheme 3. Electrochemical detection of CdS QDs "wired" by Os-PVP complex to the surface of a SPCE.

Figure

TABLE OF CONTENTS (TOC)

Modulation of Growth of Cysteine-capped Cadmium Sulphide Quantum Dots with Enzymatically produced Hydrogen Peroxide

Ruta Grinyte, Javier Barroso, Laura Saa, Valeri Pavlov*

Biofunctional Nanomaterials Unit, CIC BiomaGUNE, Parque Tecnológico de San Sebastian, Paseo Miramón 182, Donostia-San Sebastián, 20009 Spain

Page Numbers. The font is ArialMT 16 (automatically inserted by the publisher)

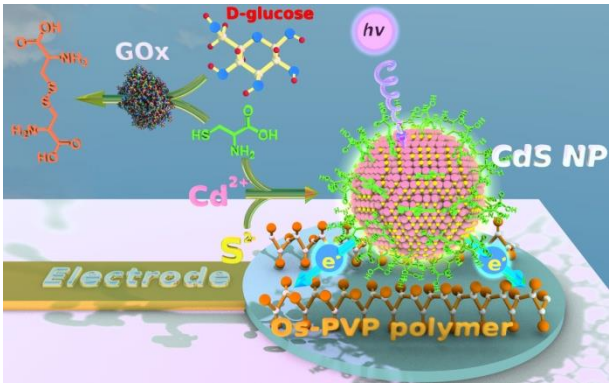

Enzymatically produced hydrogen peroxide oxidizes cysteine modulating the growth of quantum dots. This system allows quantification of glucose oxidase and glucose in human serum, using fluorescence spectroscopy and photoelectrochemical analysis.